This is to certify that the
thesis entitled

EQUILIBRIUM MICROSTRUCTURE FOR LIQUID CRYSTALLINE POLYMERS

presented by

Hemant Kamalakar Kini

has been accepted towards fulfillment
of the requirements for the

M.S. degree in Chemical Engineering & Materials Science

Charles A. Petty
Major Professor's Signature

August 19, 2003
Date

EQUILIBRIUM MICROSTRUCTURE FOR LIQUID CRYSTALLINE POLYMERS

By

Hemant Kamalakar Kini

A THESIS

Submitted to
Michigan State University
in partial fulfillment of the requirements
for the degree of

MASTER OF SCIENCE

Department of Chemical Engineering and Materials Science

2003

ABSTRACT

EQUILIBRIUM MICROSTRUCTURE FOR LIQUID CRYSTALLINE POLYMERS

By

Hemant Kamalakar Kini

The relaxation of the microstructure of liquid crystalline polymers subject to Brownian motion and a Maier-Saupe (MS-) excluded volume potential is predicted by the following dynamic equation for the second order moment of the orientation distribution:

$$\frac{d<\underline{\underline{pp}}>}{d\tau} = -(<\underline{\underline{pp}}> - \frac{1}{3}\underline{\underline{I}}) + U(<\underline{\underline{pp}}> \cdot <\underline{\underline{pp}}> - <\underline{\underline{pp}}> : <\underline{\underline{pppp}}>)$$

A recently developed algebraic closure for $<\underline{\underline{pppp}}>$, the fourth order moment of the orientation distribution function, provides a closure for the above equation.

The new theory predicts the existence of multiple equilibrium states for a MS-coefficient U between 4.656 and 5.000. At steady state, an isotropic orientation dyadic satisfies the moment equation for all values of U. The theory shows that the isotropic equilibrium microstructure is stable for $U < 4.656$ and unstable for $U > 5.000$. For $4.656 < U < 5.000$, three steady states are predicted: a conditionally stable isotropic state, an unstable anisotropic state, and a conditionally stable anisotropic state. The equilibrium semi-positive quadratic form associated with the orientation dyadic has a prolate shape (i.e., two equal eigenvalues smaller than the maximum eigenvalue). The temporal relaxation of a non-equilibrium state to an equilibrium state occurs for time scales comparable to $1 / D_R$, where D_R is a phenomenological rotary diffusion coefficient.

To my parents

ACKNOWLEDGEMENTS

My utmost gratitude to my advisor Dr Charles A. Petty for all his help, guidance and inspiration during the course of this research. It is due to his unrelenting support and prodding that I was able to complete the research and write up this thesis in the given time frame. My sincere thanks to Dr André Bénard and other members of the research group for their valuable suggestions towards my research.

I am obliged to my family and friends for their love and emotional support.

I would also like to thank the National Science Foundation (NSF/CTS-9986878) and the Department of Chemical Engineering and Materials Science for their financial support to this research.

TABLE OF CONTENTS

LIST OF TABLES

Page

LIST OF FIGURES

Page

LIST OF NOTATION

Symbol	
$\underline{\underline{a}} = \langle \underline{p}\underline{p} \rangle$	Orientation dyadic
a_{11}, a_{22}, a_{33}	Diagonal components of the orientation dayadic
$\langle \underline{p}\underline{p}\underline{p}\underline{p} \rangle$	Orientation tetradic
a_1, a_2, a_3	Eigenvalues of $\underline{\underline{a}}$
$\underline{\underline{b}}$	Anisotropic orientation dyadic
b_1, b_2, b_3	Eigenvalues of $\underline{\underline{b}}$
II_b	Second invariant of $\underline{\underline{b}}$
III_b	Third invariant of $\underline{\underline{b}}$
ψ	Probability distribution function
$\underline{n}$	Unit normal vector
$\langle \underline{p}\underline{p}\underline{p}\underline{p} \rangle$	Orientation tetradic
α	Scalar order parameter
U	Nematic strength
U_{ip}	Critical U beyond which the isotropic states are unstable
U_{pi}	U corresponding to prolate-isotropic transition
α_{ip}	α corresponding to isotopic-prolate transition
k	Boltzman constant
T	Absolute temperature
D_R	Rotary diffusion coefficient
τ	Dimensionless time

Symbol	
C_1	Coefficient of linear terms in FSQ-closure
C_2	Coefficient of quadratic terms in FSQ-closure

CHAPTER 1

BACKGROUND

1.1 Introduction

Liquid crystals are ubiquitous in the world of digital electronics in particular and in our life in general. Nematic liquid crystals can be found in display devices like laptops, calculators, watches to name a few. Cholesterics or chiral nematics (a special case of the nematic state) are used as temperature indicators in medical diagnoses or in paints to produce angle dependent iridescent colors. Smectic liquid crystals due to their layered structure, have potential application as lubricants. Liquid crystals by their structure and properties can be considered as intermediate between classical solids and classical liquids. Liquid crystals are complex fluids, which can flow like liquids but their mechanical properties are anisotropic like those of crystals. Most of the historic work on liquid crystals was with low molecular weight materials.

Liquid crystalline polymers (LCPs) are not only liquid crystalline but also viscoelastic. A polymeric mesophase (positional and/or orientational long-range order in one or two dimensions) was first discovered by Bawden and Pirie (see page 503, Larson), when they observed that, a solution of tobacco mosaic virus formed two phases above a critical concentration, one of which was birefringent. A synthetic polymer solution, poly(γ-benzyl-L-glutamate) exhibiting liquid crystalline phase, was reported in 1950 by Elliot and Ambrose (see page 1, Weiss,1990). Generally in solids the molecules possess both positional and orientational order. This means that the centers of mass of the molecules lie at specific locations and the molecular axes point in certain directions. Spherically symmetric molecules can have positional order but no orientational order.

Such positional and orientational order is absent in classical liquids. In solids, thermal motion may lead to small changes in the positions and orientations of the molecules, but their positions are in general fixed at specific lattice points and the motion is with respect to the perfect geometrical lattice. In liquids, the molecules diffuse freely and randomly in all directions. In LCPs, the molecules diffuse through the sample while still retaining some positional and orientational order. Liquid crystals exhibit long-range orientational order. A liquid crystalline phase (mesomorphic phase) can either be the result of temperature change (thermotropic), or the addition of a solvent (lyotropic). Figure 1.1 at the end of this chapter, shows the sequential progression of order for various liquid crystal phases exhibited by rod-like particles. A very common example of a lyotropic liquid crystalline polymer is 1,4-phenyleneterephthalamide, sold commercially as Kevlar. This progression wherein the liquid crystal phase is intermediate between an isotropic liquid and crystalline solid can be described by three types of order: orientational order, positional order and bond orientational order (see page 3, Collings and Patel, 1997).

The nematic phase is characterized by the long axes of the molecules, tending to align along a certain direction as they move about in the sample. This is the only long range order present in the nematic phase and hence its properties are those of an anisotropic fluid. Figure 1.2b is a schematic representation of the molecular order in a nematic phase. The molecules are represented by oblate ellipses. The ellipses can be seen to be exhibiting some average orientation; however there is no long range order in the relative positions of the ellipses. These phases are optically anisotropic and fluid-like, without any long range positional order.

The nematic liquid crystals are used in display devices, wherein their direction of preferred orientation can be switched by the application of an electric field. And with the optical properties such as birefringence strongly dependent of the orientation, the nematics can be used as optical switches. A smectic phase exhibits both positional and orientational order. Smectic phases have layered structure, and the positional order may be along the layer or between the layers. There can be three types of positional order: short range positional (SRO) order wherein the order is evident only over a finite distance as in a simple fluid; long range positional order (LRO) which is seen in a three dimensional crystal; quasi-long range order wherein the order is between that of SRO and LRO. Depending on the average orientation angle made by the molecules with the layers there can be different smectic phases. An isotropic state does not posses long range orientational order, the structure can be considered to be reminiscent of the proverbial 'bag of nails'. The liquid crystalline phases can be identified by various techniques like miscibility and optical observation of textures, the most comprehensive understanding of the molecular order can be attained by the X-ray diffraction studies on oriented samples.

As in LCPs, the behavior of rigid rod like particles dispersed in a viscous fluid is of great importance in the processing of composite materials. Due to their low cost, fast cycle times and good mechanical properties, the use of composites has increased tremendously over the years. Many composite materials are formed, by combining a reinforcing fiber with a polymeric or metallic matrix. These materials are processed in different ways depending on the type of reinforcement used and the fiber orientation in the final composite, which influences the final composite mechanical properties. As the composite is being formed, flow induces the fibers to be oriented, this orientation

template is retained in the finished product. This fiber orientation template in the composite material controls its mechanical properties. The direction in which most of the fibers are oriented is stronger and stiffer than the direction with the least orientation (see Advani and Tucker 1987; Parks *et al.* 1999; Tucker, 1988).

There are both theoretical and experimental models for correlating the mechanical properties with the direction of fiber orientation. Hence there is an ample incentive for understanding the complex link between the composite manufacturing process, the final fiber orientations and the composite properties. This knowledge would allow one to design and control the process to obtain the most desirable mechanical properties in the composite material. Predicting full-scale processing flows, where the flow is inhomogeneous, necessitates tracking of all the particles, which is a tedious task. In polymeric liquids, any molecule experiences an average effect of its surroundings and the problem reduces to calculating the mean properties from the behavior of individual molecules. Though these assumptions simplify the problem, they are made while retaining enough information to extract accurate predictions of the rheology and molecular orientation (see Folgar and Tucker, 1984; Advani and Tucker 1987).

The change in concentration of rigid rod like polymers causes dramatic changes in the rheological properties of LCPs and other polymeric solutions. Onsager and Flory (see page 229, Doi, 1981) identified critical concentration for solutions of such molecules, above which they form liquid crystals with a nematic structure. This theoretical prediction can be validated by viscosity measurements and polarized light microscopy of the microstructure of polyisocyanates as done by Aharoni (1979,1980). Both these studies have shown the existence of a critical concentration of the polymer above which

there is a transition from isotropic state to an anisotropic state, as the polymer concentration is increased. The phenomenological theory of Ericksen, Leslie and Parodi (see page 229, Doi, 1981), was successful in describing many dynamical phenomena in nematic, thermotropic liquid crystals. But this theory does not predict the nonlinear viscoelasticity, which is quite conspicuous in such systems. Doi (1981), proposed a model based on molecular approach, which predicted a nonlinear viscoelasticity for LCPs. Also the predicted dependence of the viscosity on molecular weight and concentration agreed fairly well with experiments.

Using the fluids microstructure numerous fluid mechanical theories have been formulated. Jeffery (1922), studied the fluid motion in the vicinity of a suspended ellipsoid to explain the increase in viscosity due to its presence, in an otherwise Newtonian fluid. For a suspension of non-interacting dumbbell shaped particles, Prager (see page 33, Hand, 1961) deduced a constitutive equation for stress and equations determining the preferred direction adopted by the particles. The orientation state of the fibers can be represented in numerous ways. The probability distribution function for the fibers is one way (see Advani and Tucker, 1990,1994; Cintra and Tucker, 1995). It is suitable for problems involving nontrivial flow fields with planar orientation. A more compact way of representing the fiber orientation is by using various parameters. The formulation of these parameters depends on assumptions about the direction of the principal axes of orientation and some symmetry in the probability distribution function. An ideal description of fiber orientation would be general like the distribution function and compact like orientation parameters. These requirements are satisfied by a set of tensors that have been called tensorial order parameters or orientation-moment tensors.

The underlying theory for this research utilizes this form of representation for the orientation state, as suggested by Hand (1962) and the Doi (seee Doi and Edwards, 1986) theory for liquid crystalline polymers. The tensorial form of description while providing an efficient way to compute flow-induced fiber orientation, requires an accurate closure approximation for the higher-order moments of the orientation distribution function. Over the years several closure approximations have been proposed, some of which are discussed later.

1.2 Characterization of the Microstructure

1.2.1 Orientation Characterization and Distribution

The polymer molecule is considered to be a rigid rod uniform in length and diameter. The two ends of this polymer are identical. The orientation of this molecule can be represented by an unit vector $\underline{p}$, directed along its molecular axis or by angles θ and ϕ made by the molecular axis. Fig 1.3 shows these forms of representation. The two forms of representation are related by,

$$p_1=\sin\theta\cos\phi \qquad p_2=\cos\theta \qquad p_3=\sin\theta\sin\phi \ . \qquad (1.1)$$

p_1 , p_2 , p_3 are the components of the unit vector $\underline{p}$ along the co-ordinate axes X,Y and Z respectively.

As the 'head' and 'tail' of the molecule are indistinguishable from each other, the representation of the polymer direction is unchanged by changing $\underline{p}$ to $-\underline{p}$ or θ and ϕ as below

$$\theta \longrightarrow \pi-\theta \qquad \phi \longrightarrow \pi+\phi \ . \qquad (1.2)$$

A probability distribution function $\psi\ (\theta,\phi)$ describes the orientation state of a particle in space, it is the fraction of orientation states per unit area on a sphere of unit radius. The probability P, of finding a particle between θ_1 and $\theta_1 + \Delta\theta$; and ϕ_1 and $\phi_1 + \Delta\phi$ is given by

$$P\ (\theta \le \theta \le \theta + \Delta\theta\ ,\ \phi \le \phi \le \phi + \Delta\phi) = \psi\ (\theta,\phi)\ \sin\theta\ \Delta\theta\ \Delta\phi\ . \tag{1.3}$$

This function is normalized by integrating the function over the entire sphere i.e., the probability of finding a particle at some orientation over the sphere is unity,

$$\iint \psi\ (\theta, \phi, t)\ \sin\ \theta\ d\theta\ d\phi\ = 1\quad . \tag{1.4}$$

From the definition of $\underline{p}$ we can write that

$$\psi(\underline{p})\ = \psi(-\underline{p}) \tag{1.5}$$

$$\psi(\theta,\phi)\ = \psi(\pi - \theta, \phi + \pi) \qquad . \tag{1.6}$$

1.2.2 Continuity Equation

Considering an arbitrary area over the unit sphere, as shown in Figure 1.4. This area is bounded by the contour line C. Relative to a material frame of reference, the flux of the orientation states across the boundary C is $\dot{\underline{p}}\,\psi$. Writing a balance of orientation states across the surface A,

$$-\int_C (\dot{\underline{p}}\,\psi)\cdot\underline{n}\ ds\ =\ \frac{d}{dt}\iint_A \psi(\theta, \phi, t)\ dA \qquad . \tag{1.7}$$

Using Stokes theorem (see Deen, 1998), the left-hand-side of Eq. (1.7) can be written as,

$$-\int_{c}(\dot{\underline{p}}\,\psi)\cdot\underline{n}\,ds \equiv \iint_{A}\frac{\partial}{\partial\underline{p}}\cdot(\dot{\underline{p}}\,\psi)\,dA \quad . \tag{1.8}$$

The equation for the evolution of ψ for the spatially homogeneous LCP mixture can be written as,

$$\frac{\partial\psi}{\partial t}=-\frac{\partial}{\partial\underline{p}}\cdot(\dot{\underline{p}}\,\psi) \quad . \tag{1.9}$$

The term $(\dot{\underline{p}}\,\psi)$ represents the rotary flux, where $\dot{\underline{p}}$ is the angular velocity of the LCP component and $\frac{\partial}{\partial\underline{p}}$ is the surface gradient operator. The rotary flux can now be written as the contributions from convective and diffusive fluxes,

$$\dot{\underline{p}}\,\psi \equiv \dot{\underline{p}}_{c}\,\psi+(\dot{\underline{p}}\,\psi-\dot{\underline{p}}_{c}\psi) \quad . \tag{1.10}$$

$\dot{\underline{p}}_{c}$ is the angular velocity caused by fiber/fluid interactions .

Now Eq. (1.9) can be written in terms of the convective and diffusive fluxes

$$\frac{\partial\psi}{\partial t}=-\frac{\partial}{\partial\underline{p}}\cdot(\dot{\underline{p}}_{c}\psi)-\frac{\partial}{\partial\underline{p}}\cdot(\dot{\underline{p}}-\dot{\underline{p}}_{c}\psi) \quad . \tag{1.11}$$

1.2.3 Rotary Diffusive Flux

The rotary diffusive flux has a contribution due to Brownian motion and a contribution due to an excluded volume potential :

$$(\dot{\underline{p}} - \dot{\underline{p}}_c)\psi = -D_R\left[\frac{\partial \psi}{\partial \underline{p}} + \psi \frac{\partial}{\partial \underline{p}}\left(\frac{\Delta U_{MS}}{k_B T}\right)\right] \quad , \tag{1.12}$$

where D_R is the rotary diffusion coefficient and has the units of 1/time.

1.2.3.1 Maier-Saupe potential

Orientation distribution can be calculated from a nematic potential which signifies the influence of one molecule or a rod's orientation on that of its neighbor. Every polymer molecule has a region around it wherein the stearic effect precludes other molecules from that region. This is called the excluded volume. Onsager initially proposed a theory to calculate such a potential. This theory is applicable at low concentrations at which pairwise excluded volume interactions are the dominant ones. The Doi theory utilizes the Maier-Saupe potential ΔU_{MS}, which is more suitable for thermotropic nematics.

$$\Delta U_{MS} = -\frac{3}{2} U k_B T (\underline{\underline{pp}} - \frac{1}{3}\underline{\underline{I}}) : (\underline{\underline{pp}} - \frac{1}{3}\underline{\underline{I}}) \; . \tag{1.13}$$

U is a dimensionless measure of the polymer number density n and is directly proportional to the excluded volume between rigid rods. When the concentration of the polymer is increased, the interaction forces become stronger, this increases the alignment

of polymer molecules. Hence there can be a transition from a random to an ordered phase even in the absence of flow.

1.3 Dynamic Equation for the Orientation Dyadic

1.3.1 The Smoluchowski Equation

The Smoluchowski equation with $\dot{\underline{p}}_c = 0$ (no external flow field), can be written as

$$\frac{\partial \psi}{\partial t} = D_R \frac{\partial}{\partial \underline{p}} \cdot [\frac{\partial \psi}{\partial \underline{p}} + \psi \frac{\partial}{\partial \underline{p}} (\frac{\Delta U_{MS}}{k_B T})] \ . \tag{1.14}$$

The Smoluchowski equation gives the evolution of the orientation distribution function. Multiplying Eq. (1.14) by $\underline{p}\,\underline{p}$ and integrating the equation over the entire unit sphere gives

$$\frac{d < \underline{p}\underline{p} >}{d\tau} = -(< \underline{p}\,\underline{p} > - \frac{1}{3}\underline{\underline{I}}) + U(< \underline{p}\,\underline{p} > \cdot < \underline{p}\,\underline{p} > - < \underline{p}\,\underline{p} > : < \underline{p}\,\underline{p}\,\underline{p}\,\underline{p} >) \ , \tag{1.15}$$

where $\tau \equiv 6 D_R t$ is the dimensionless time.

1.4 Closure models for orientation tetradic

1.4.1 Background

As evident from the earlier discussion the distribution function $\psi(\theta, \phi, t; U)$ provides a description of the fiber orientation state. A compact representation of the orientation for numerical simulations is in the form of orientation tensors. The dyadic product of the vector $\underline{p}$ with itself and the integration of this product, with the

distribution function over all possible directions, yields one set of orientation tensor. As the distribution function is even, the odd order integrals are zero. The integrals of importance are the even-ordered ones (see Imhoff, 2000). The second order tensor or dyad can be written as

$$< \underline{p}\,\underline{p} >= \iint \underline{p}\,\underline{p}\,\psi\,(\theta,\phi,t)\sin\theta\;d\theta\,d\phi \quad . \tag{1.16}$$

Similarly the fourth order tensor or tetrad is

$$< \underline{p}\,\underline{p}\,\underline{p}\,\underline{p} >= \iint \underline{p}\,\underline{p}\,\underline{p}\,\underline{p}\,\psi\,(\theta,\phi,t)\sin\theta\;d\theta\;d\phi \quad . \tag{1.17}$$

The fourth order tensor must reduce to the second order tensor by contracting any two orientation vectors:

$$\begin{aligned} < p_i p_j > &= < p_s p_s p_i p_j > = < p_s p_i p_s p_j > = < p_s p_i p_j p_s > \\ &= < p_i p_s p_s p_j > = < p_i p_s p_j p_s > = < p_i p_j p_s p_s > \end{aligned} \tag{1.18}$$

Clearly, the orientation tetrad also has six fold symmetry inasmuch as

$$\begin{aligned} < p_i p_j p_k p_l > &= < p_i p_j p_k p_l > = < p_i p_k p_j p_l > = < p_i p_l p_j p_k > \\ &= < p_k p_l p_i p_j > = < p_j p_l p_i p_k > = < p_j p_k p_i p_l > \end{aligned} \tag{1.19}$$

An infinite number of even order tensors can be written. The higher the number of orientation tensor, the better is the description of the orientation state. But the calculation of higher order tensors is very cumbersome. Hence the second and fourth order tensors which provide an adequate representation of the orientation state are commonly used.

When the equation for $<\underline{p}\underline{p}>$ is written, it has the higher order moment $<\underline{p}\underline{p}\underline{p}\underline{p}>$, which needs to be determined. Whenever an equation for any finite moment of $\underline{p}$ is written, it will always contain a higher order moment of $\underline{p}$. So to solve for $<\underline{p}\underline{p}>$, we need to close the higher order moment $<\underline{p}\underline{p}\underline{p}\underline{p}>$. Some of the commonly used closures and the closure used in this research (i.e., the FSQ- closure) are now discussed.

1.4.2 The linear closure model of Hand

This linear closure proposed by Hand (1962) is given by

$$<\underline{p}\underline{p}\underline{p}\underline{p}>:<\underline{p}\underline{p}>=[(-\frac{1}{35}+\frac{1}{7}<\underline{p}\underline{p}>:<\underline{p}\underline{p}>)\underline{\underline{I}}+\frac{3}{35}<\underline{p}\underline{p}>+\frac{4}{7}<\underline{p}\underline{p}>\cdot<\underline{p}\underline{p}>] \tag{1.20}$$

This closure satisfies all the projection and symmetry properties of the exact orientation dyadic. The predictions made by this model are found to be accurate near the isotropic state.

1.4.3 The uncoupling approximation

The uncoupling approximation which was first used by Doi (1981), is

$$<\underline{p}\underline{p}\underline{p}\underline{p}>:<\underline{p}\underline{p}>=<\underline{p}\underline{p}>(<\underline{p}\underline{p}>:<\underline{p}\underline{p}>)\ . \tag{1.21}$$

This is one of the simplest closures and has been widely used to describe LCPs. Here the fourth order moment is expressed as the product of the first order dyads. For simple shear flows, this approximation fails to show the director tumbling and wagging transitions predicted by the unapproximated Doi theory (see Feng *et al.* ,(1998)).

1.4.4 The quadratic closure of Hinch and Leal (HL1 closure)

This closure was proposed by Hinch and Leal (1975,1976). Hinch and Leal developed a closure for the orientation tetrad by interpolating between two regimes: near equilibrium (weak flows) flows and strong-flows.

$$\begin{aligned}<\underline{p}\underline{p}\underline{p}\underline{p}>:<\underline{p}\underline{p}> \;=& \frac{1}{3}<\underline{p}\underline{p}>+\frac{1}{5}(6<\underline{p}\underline{p}>\cdot<\underline{p}\underline{p}>\cdot<\underline{p}\underline{p}>-2<\underline{p}\underline{p}>\cdot<\underline{p}\underline{p}> \\ & -<\underline{p}\underline{p}><\underline{p}\underline{p}>:<\underline{p}\underline{p}>+\frac{1}{3}<\underline{p}\underline{p}><\underline{p}\underline{p}>:\underline{\underline{I}}+2\underline{\underline{I}}<\underline{p}\underline{p}>:<\underline{p}\underline{p}> \\ & -\frac{2}{3}\underline{\underline{I}}<\underline{p}\underline{p}>:\underline{\underline{I}}-2\,\underline{\underline{I}}<\underline{p}\underline{p}>\cdot<\underline{p}\underline{p}>:<\underline{p}\underline{p}>+\frac{2}{3}\underline{\underline{I}}<\underline{p}\underline{p}>\cdot<\underline{p}\underline{p}>:\underline{\underline{I}})\end{aligned} \tag{1.22}$$

The accuracy of the closure varies considerably when applied to the excluded volume term $<\underline{p}\underline{p}>:<\underline{p}\underline{p}\underline{p}\underline{p}>$ and the flow term $\underline{\underline{S}}:<\underline{p}\underline{p}\underline{p}\underline{p}>$, where $\underline{\underline{S}}$ is the strain rate dyadic. The quadratic closure is found to be more accurate than the HL1 closure for the nematic term, while the HL1 closure is found to be more accurate than the quadratic closure for the flow term.

1.4.5 The fully symmetric quadratic (FSQ-) closure

This closure was proposed by Petty *et al.* (1999). This closure has a linear and a quadratic part, and is defined as follows

$$<\underline{p}\underline{p}\underline{p}\underline{p}>=C_1<\underline{p}\underline{p}\underline{p}\underline{p}>_1+C_2<\underline{p}\underline{p}\underline{p}\underline{p}>_2 \tag{1.23}$$

$$<\underline{p}\underline{p}\underline{p}\underline{p}>_1:<\underline{p}\underline{p}>=[(-\frac{1}{35}+\frac{1}{7}<\underline{p}\underline{p}>:<\underline{p}\underline{p}>)\underline{\underline{I}}+\frac{3}{35}<\underline{p}\underline{p}>+\frac{4}{7}<\underline{p}\underline{p}>\cdot<\underline{p}\underline{p}>] \tag{1.24}$$

$$< \underline{p}\underline{p}\underline{p}\underline{p} >_2 :< \underline{p}\underline{p} > = [(\frac{2}{35} < \underline{p}\underline{p} >:< \underline{p}\underline{p} > - \frac{2}{7}\mathrm{tr}(< \underline{p}\underline{p} > \cdot < \underline{p}\underline{p} > \cdot < \underline{p}\underline{p} >))\underline{\underline{I}} +$$
$$(\frac{39}{35} < \underline{p}\underline{p} >:< \underline{p}\underline{p} >) < \underline{p}\underline{p} > - \frac{2}{7} < \underline{p}\underline{p} > \cdot < \underline{p}\underline{p} > + \frac{6}{7} < \underline{p}\underline{p} > \cdot < \underline{p}\underline{p} > \cdot < \underline{p}\underline{p} >] \tag{1.25}$$

The linear part of the closure i.e., $< \underline{p}\underline{p}\underline{p}\underline{p} >_1$ is identical to the Hand closure. The closure retains the six fold symmetry and projection properties of the exact orientation tetradic. The tetradics $< \underline{p}\underline{p}\underline{p}\underline{p} >_1$ and $< \underline{p}\underline{p}\underline{p}\underline{p} >_2$, individually satisfy the six fold symmetry and projection properties. The projection property for Eq. (1.23) is recovered by requiring

$$C_1 + C_2 = 1. \tag{1.26}$$

At the nematic state $C_2 = 1/3$ (see Appendix D). Eq. (1.23) can be written as,

$$< \underline{p}\underline{p}\underline{p}\underline{p} >:< \underline{p}\underline{p} > = \frac{2}{3}[(-\frac{1}{35} + \frac{1}{7} < \underline{p}\underline{p} >:< \underline{p}\underline{p} >)\underline{\underline{I}} + \frac{3}{35} < \underline{p}\underline{p} > + \frac{4}{7} < \underline{p}\underline{p} > \cdot < \underline{p}\underline{p} >]$$
$$+ \frac{1}{3}[(\frac{2}{35} < \underline{p}\underline{p} >:< \underline{p}\underline{p} > - \frac{2}{7}\mathrm{tr}(< \underline{p}\underline{p} > \cdot < \underline{p}\underline{p} > \cdot < \underline{p}\underline{p} >))\underline{\underline{I}} +$$
$$(\frac{39}{35} < \underline{p}\underline{p} >:< \underline{p}\underline{p} >) < \underline{p}\underline{p} > - \frac{2}{7} < \underline{p}\underline{p} > \cdot < \underline{p}\underline{p} > + \frac{6}{7} < \underline{p}\underline{p} > \cdot < \underline{p}\underline{p} > \cdot < \underline{p}\underline{p} >] \tag{1.27}$$

The FSQ-closure satisfies the six fold symmetry and contraction properties discussed in Section 1.4.1.

1.5 Objectives

Equation (1.15) determines the evolution of the orientation dyadic. Solving the differential equation requires the evaluation of the term $< \underline{pp} >:< \underline{pppp} >$. This term, can be evaluated by the various closure models discussed earlier and the FSQ-closure (see Section 1.4.5).

In this research the following characteristics of Eq. (1.15) are examined:
1) the critical vales of U for the transitions between the liquid crystalline phases ; 2) the equilibrium microstructure and phase transitions for lyotropic LCPs using the FSQ-closure ; and 3) the predictions made by the uncoupling approximation and the HL1 closure.

1.6 Methodology

The second order orientation moment satisfies Eq. (1.15) .The FSQ-closure, which satisfies the above conditions, is used to calculate the fourth order orientation moment $<\underline{pppp}>$. The goal of the simulations is to predict the critical concentrations for the transitions between the different prolate and isotropic states, and to get the equilibrium phase diagram. Figure 1.5 shows a typical equilibrium phase diagram with the different prolate and isotropic states. The arrows "a" and "b" indicate the transition between the conditionally stable prolate states to the conditionally stable isotropic and stable prolate states respectively. The other arrows, as marked, show the prolate-isotropic and isotropic-prolate transition. The equilibrium orientation states depend on the value of U. Below the U_{pi}, the microstructure relaxes to a stable isotropic state. Beyond U_{ip}, the isotropic states are unstable, while the prolate states are all stable. Between U_{pi} and U_{ip}, the isotropic and

prolate states are conditionally stable. The faint curve represents the transition between conditionally stable isotropic and prolate states (i.e, finite perturbation of a microstructure on the faint line will change the microstructure to either the conditionally stable prolate state or the isotropic state). As U is increased beyond U_{ip} the microstructure gets increasingly oriented in one direction (i.e, it tends towards the nematic state). However, Brownian motion of the solvent molecules prevents the dispersed phase from becoming nematic for $U < \infty$.

1.6.1 Prolate-Isotropic transition U_{pi}

Eq. (1.15) is solved using a fourth order Runge-Kutta algorithm (see Matlab code in Appendix H) subject to the following conditions for $0 < \tau \leq 800$:

$$< \underline{p}\,\underline{p} >_0 = \underline{e}_3\,\underline{e}_3 \ .$$

The temporal step size $\Delta\tau = 0.01$.

The simulations are started with U=1. The nematic state (initial state) corresponds to point A on the invariant diagram (see Figure A.1, Appendix A). At the end of the simulation $a_{33}(\tau)$ is plotted as a function of the dimensionless time, τ. This gives the visual conformation that the orientation state is fully relaxed to a steady state. At the isotropic state the orientation dyadic has the form,

$$< \underline{p}\,\underline{p} > = \frac{1}{3}[\underline{e}_1\underline{e}_1 + \underline{e}_2\underline{e}_2 + \underline{e}_3\underline{e}_3] \ .$$

The calculation is repeated for larger values of U. At a particular value of $U=U_{ip}$, the nematic state relaxes to an anisotropic state (see Figure 1.5). At values of U less than U_{pi} the nematic state relaxes to a stable isotropic state. This is the region of stable

isotropic states. For $U \geq U_{ip}$, the nematic state relaxes to a stable prolate state. The prolate state has the form

$$<\underline{p}\underline{p}> = a_{11}\underline{e}_1\underline{e}_1 + a_{22}\underline{e}_2\underline{e}_2 + a_{33}\underline{e}_3\underline{e}_3 \ .$$

where $a_{11} = a_{22} < a_{33}$.

1.6.2 Isotropic-prolate transition, U_{ip}

For $U > U_{ip}$, the isotopic state is unstable. To locate this point for a particular value of U beyond U_{ip}, the simulation is started with an initial state very close to the isotropic state, with a step size of 0.001 for a few hundred time steps. If the microstructure tends to relax back to the isotropic state, then the calculation is repeated with a slightly higher value of U. This is continued until $U=U_{ip}$, beyond which the microstructure tends to relax to the prolate state from an initial state close to the isotropic state as well as from the nematic state.

1.6.3 Region of multiple steady states $U_{pi} < U < U_{ip}$

To identify the region of multiple steady states, the simulations are run similar to the ones developed to identify U_{ip}. An initial state close to the isotropic state is selected. As illustrated in Figure 1.5, if the initial state is at Point "a" for a value of U between U_{ip} and U_{pi} , then it relaxes to the isotropic state. If it is at Point "b", then it relaxes to the prolate state. The simulations are repeated till the points "a" and "b" merge to yield the conditionally stable prolate and conditionally stable isptropic states between U_{pi} and U_{ip} .

1.7 Scope

C_2 is the coefficient of the quadratic terms in the FSQ-closure (see Eq. (1.23)). This research examines the influence of C_2 on the predictions made by the FSQ-closure. C_2 is equal to 1/3 at the nematic state. Two other values of C_2 = 0.29 and 0.31 are used for this purpose. The relaxation of the microstructure from an initial state is studied by varying U between 0 and 15. U= 0 corresponds to relaxation due to Brownian motion. As the value of U increases the contribution of the excluded volume increases. The relaxation times for different values of U are compared.

1.8 Figures

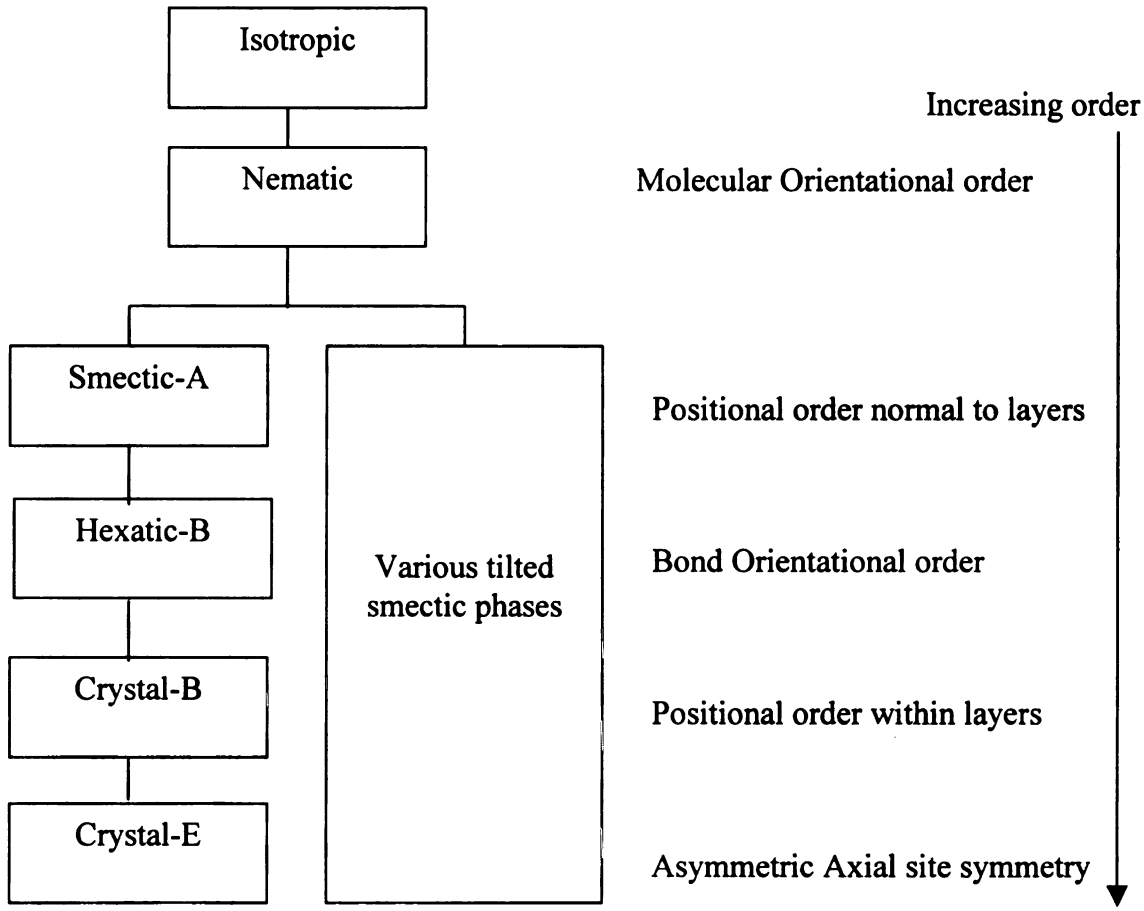

Figure 1.1. Progression of order for liquid crystal phases formed by rod like molecules.

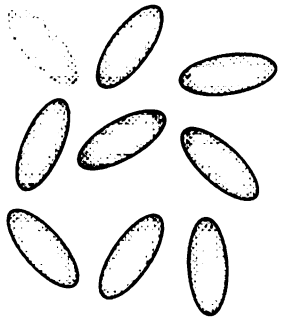

Figure 1.2a Isotropic phase

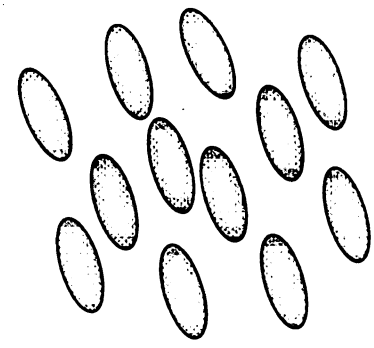

Figure 1.2b Nematic phase

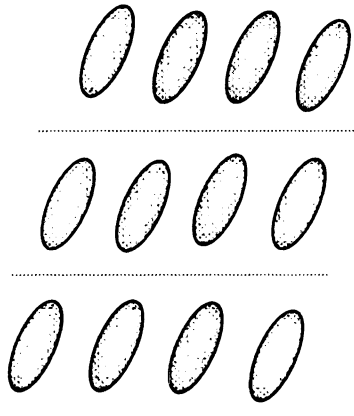

Figure 1.2c Smectic phase

Showing order between layers

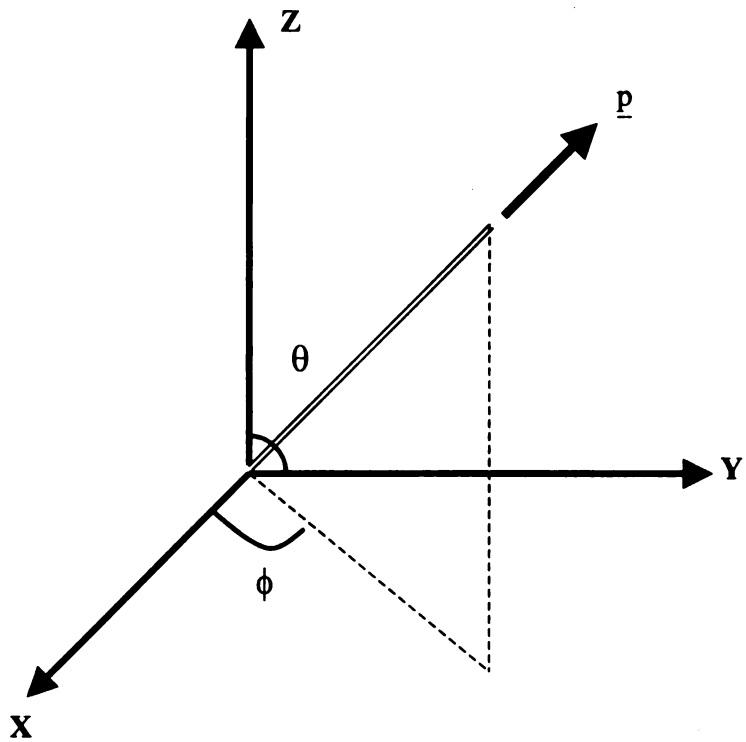

$$\underline{p} = p_1 \underline{e}_1 + p_2 \underline{e}_2 + p_3 \underline{e}_3$$

$$\underline{p} = (\sin\theta\cos\phi)\underline{e}_1 + (\cos\theta)\underline{e}_2 + (\sin\theta\sin\phi)\underline{e}_3$$

Figure 1.3 Representation of an axisymmetric polymer molecule

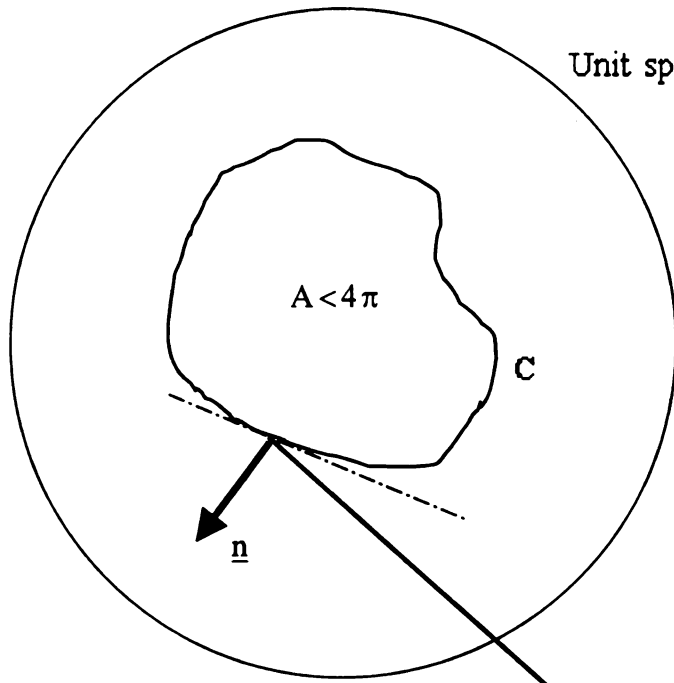

rotary flux of orientation states in a material frame of reference

$$-\int_C (\dot{\underline{p}}\,\psi)\cdot\underline{n}\,ds \;=\; \frac{d}{dt}\iint_A \psi(\theta,\phi,t)\,dA$$

loss of orientation states from area A per in A unit time due to fiber/fluid and fiber/fiber interactions

accumulation of orientation states in area A

Figure 1.4 Orientation vector distribution over the unit sphere

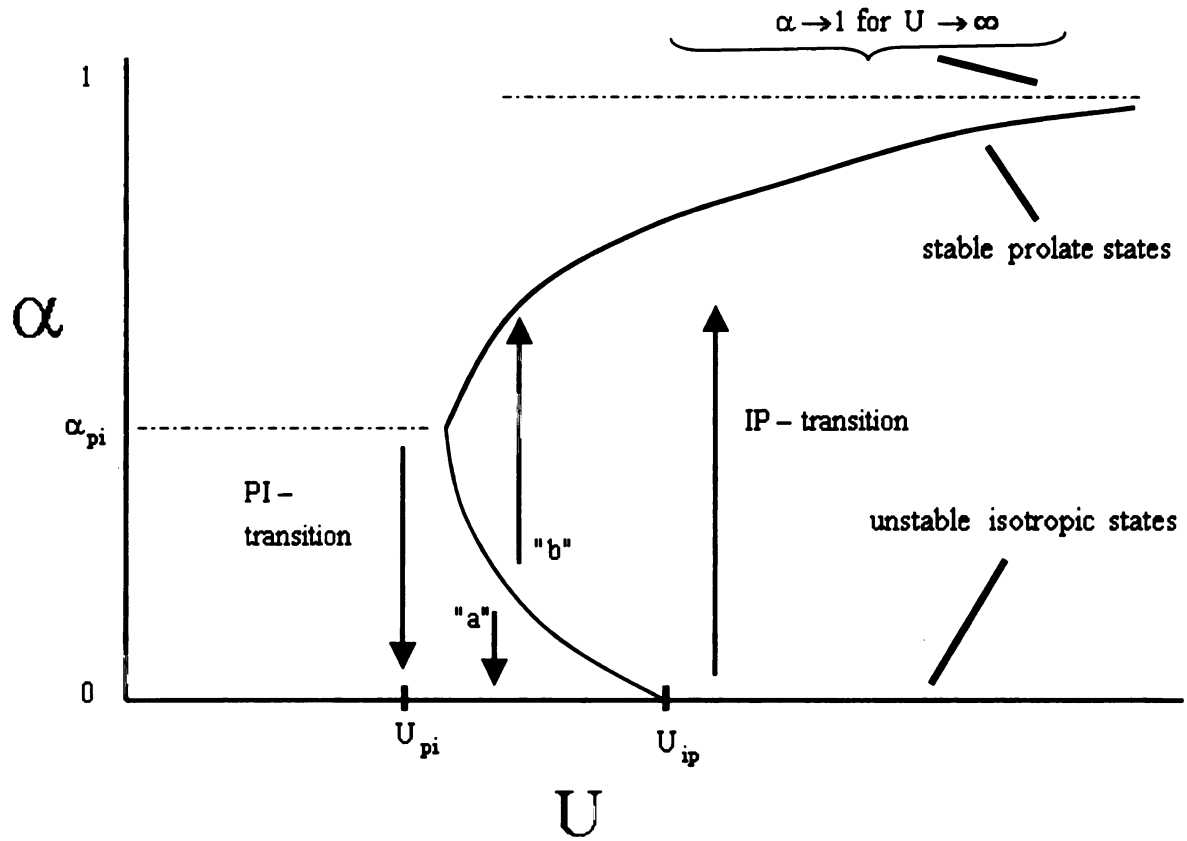

Figure 1.5 Equilibrium phase diagram indicating the prolate-isotropic transition and the isotropic-prolate transition. For definition of α see Appendix B.

CHAPTER 2

RESULTS

2.1 Steady States and Equilibrium States

The evolution equation for the second order moment (see Eq. (1.15)) is

$$\frac{D<\underline{\underline{pp}}>}{D\tau} = -(<\underline{\underline{pp}}> - \frac{1}{3}\underline{\underline{I}}) + U(<\underline{\underline{pp}}> \cdot <\underline{\underline{pp}}> - <\underline{\underline{pp}}> : <\underline{\underline{pppp}}>$$

The following properties of the orientation dyadic $<\underline{\underline{pp}}>$ must be preserved :

1) The trace of the orientation dyadic predicted must also be 1 for all $\tau > 0$.

2) The orientation dyadic $<\underline{\underline{pp}}>$ is symmetric. For this to be true at all times, the orientation tetradic $<\underline{\underline{pppp}}>$ must also have the symmetry properties (see Eq.(1.19)).

The FSQ-closure, which satisfies the above conditions, is used to calculate the fourth order moment $<\underline{p}\,\underline{p}\,\underline{p}\,\underline{p}>$. This differential equation is solved as explained in the earlier chapter. The relaxation of the microstructure is predicted with C_2= 0.29, 0.31 and 1/3.

2.1.1 Determining the point of prolate-isotropic transition,U_{ip} with $C_2 = 1/3$

The differential equation, Eq. (1.15) is solved with $C_2 = 1/3$ and other conditions described in Section 1.6. The initial run of simulation is started with U = 1. At this value of U = 1, the microstructure relaxes to an isotropic state. The simulations are repeated with a higher value of U and other conditions remaining unchanged, if the microstructure relaxes to an isotropic state. At $U_{pi} = 4.656$, the microstructure relaxes to a stable prolate state. At this point, α=0.2257 and

$$<\underline{p}\underline{p}> = \begin{bmatrix} 0.2581 & 0 & 0 \\ 0 & 0.2581 & 0 \\ 0 & 0 & 0.4838 \end{bmatrix}.$$

U_{pi} corresponds to the point of prolate-isotropic transition.

2.1.2 Determining the point of isotropic-prolate transition, U_{ip} with $C_2 = 1/3$

Eq. (1.15) is solved with $C_2 = 1/3$ and other conditions described in Section 1.6. To locate this point $U_{ip} = 4.6$, the simulation is started with an initial state $\alpha = 0.05$. This corresponds to the orientation dyadic,

$$<\underline{p}\underline{p}> = \begin{bmatrix} 0.3167 & 0 & 0 \\ 0 & 0.3167 & 0 \\ 0 & 0 & 0.3666 \end{bmatrix}.$$

The components of $<\underline{p}\underline{p}>$ are calculated from α as follows,

$$<\underline{p}\underline{p}>_{3,3} = \frac{\alpha + 1/2}{3/2}$$

$$<\underline{p}\underline{p}>_{1,1} = <\underline{p}\underline{p}>_{2,2} = \frac{1 - <\underline{p}\underline{p}>_{3,3}}{2}$$

If the microstructure tends (i.e., α becomes less than 0.05) to relax back to the isotropic state then the calculation is repeated with a slightly higher value of U. This is continued until $U = U_{ip}$, beyond which the microstructure tends (i.e., α becomes greater than 0.05) to relax to the prolate state form an initial state α=0.05. This is the point of stable-unstable isotropic transition, U_{ip}.

2.1.3 Determining the region of multiple steady states $U_{pi} < U < U_{ip}$ with $C_2 = 1/3$

The purpose of the calculations is to determine an α (conditionally stable prolate state) for the value of U lying between U_{pi} and U_{ip}. This is demonstrated by calculating α for a particular value U = 4.7. The calculations are done as follows :

Step 1. With U = 4.7 and α=0.1 as the initial condition, the microstructure tends to relax to the isotropic state.

Step 2. With U = 4.7 and α=0.2 as the initial condition, the microstructure tends to relax to the prolate state.

Step 3. With U = 4.7 , α is varied between 0.1 and 0.2 as limits. At α=0.129, the microstructure does not show a tendency to relax to the isotropic state or to the stable prolate state. α=0.129 is taken to be the conditionally stable prolate state corresponding to U=4.7.

Therefore, this method is repeated for discrete values of U between U_{ip} and U_{pi}, to determine the conditionally stable prolate region, as indicated by the dashed lines on Figure 2.1.

2.2 Relaxation to Equilibrium

As evident from Figure 2.7, the time needed for the microstructure to relax from an initial nematic state to an equilibrium isotropic state (U < 4.656 with C_2=1/3) is considerably longer for values of U which are closer to U_{pi} = 4.656 than for values of U which are considerably less than U_{pi}=4.656. This can be attributed to the microstructure trying to reach an equillibrium between the competing Brownian forces (tending to make the microstructure isotropic) and the excluded volume potential (tending to align the microstructure). At U=0 there is no excluded volume potential. The relaxation of the

microstructure is entirely due to the Brownian motion. Beyond U_{ip}, when the excluded volume potential dominates the Brownian forces the relaxation time is relatively short for the values of U close to U_{ip}.

For U lying between U_{ip} and U_{pi} there are multiple steady states. Figure 2.9 shows the multiple steady states for U=4.7, which lies between U_{pi}= 4.6556 and U_{ip} =5.0. α=0.129 corresponds to the conditionally stable prolate state. So any microstructure with α higher or lower than α=0.129 will relax to the stable prolate state (α=0.2869) and isotropic state (α=0) respectively.

Figure 2.10 shows the relaxation pathways for different initial states (α= 1, 0.15,0.05) with U=6.0 and C_2=1/3. α= 0.15 and 0.05 are initial states, which are close to the isotropic state. Since U=6 is greater than U_{ip} =5 , small perturbation from the isotropic states will take them to a stable prolate state. This state can also be reached by relaxing from an initial nematic state with the same value of U.

2.3 Figures

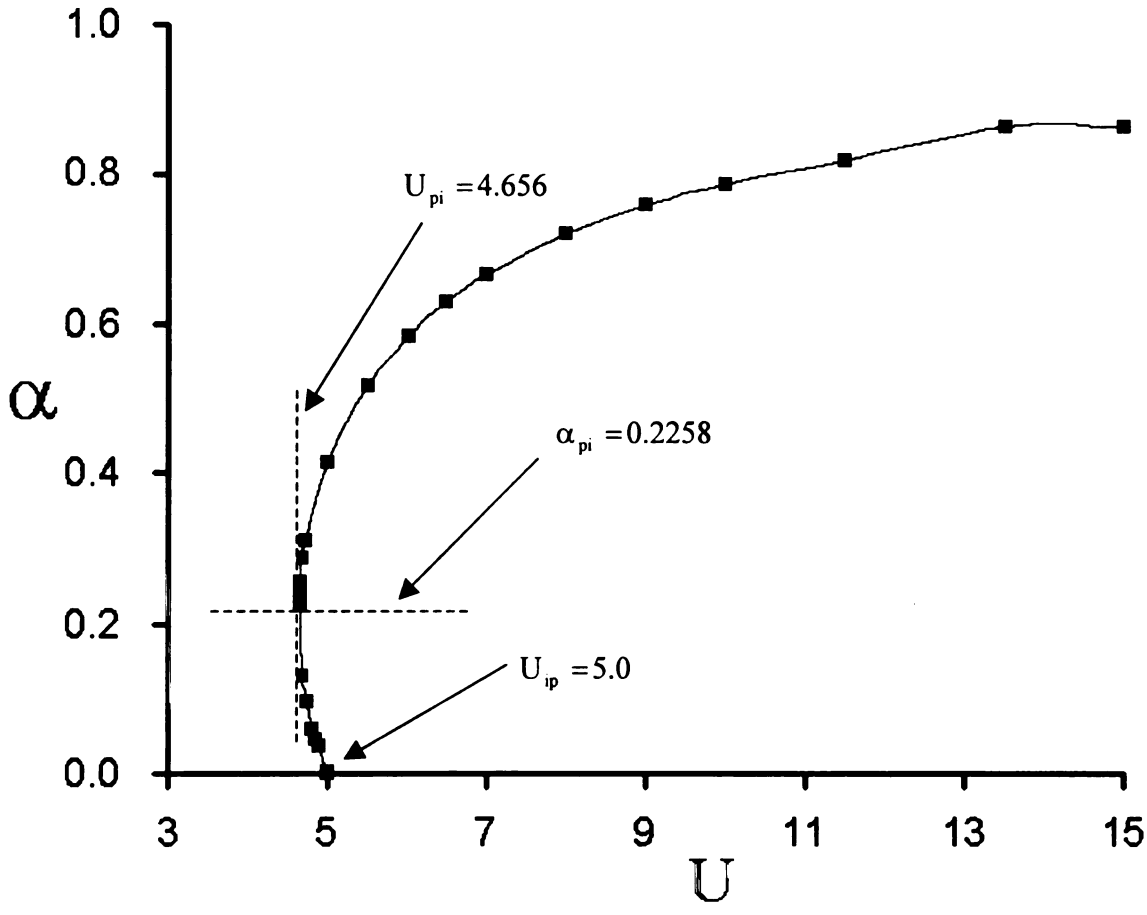

Figure 2.1 The isotropic-prolate transition predicted by the FSQ-closure with C_2=1/3. see Appendix E for the numerical values for the graph.

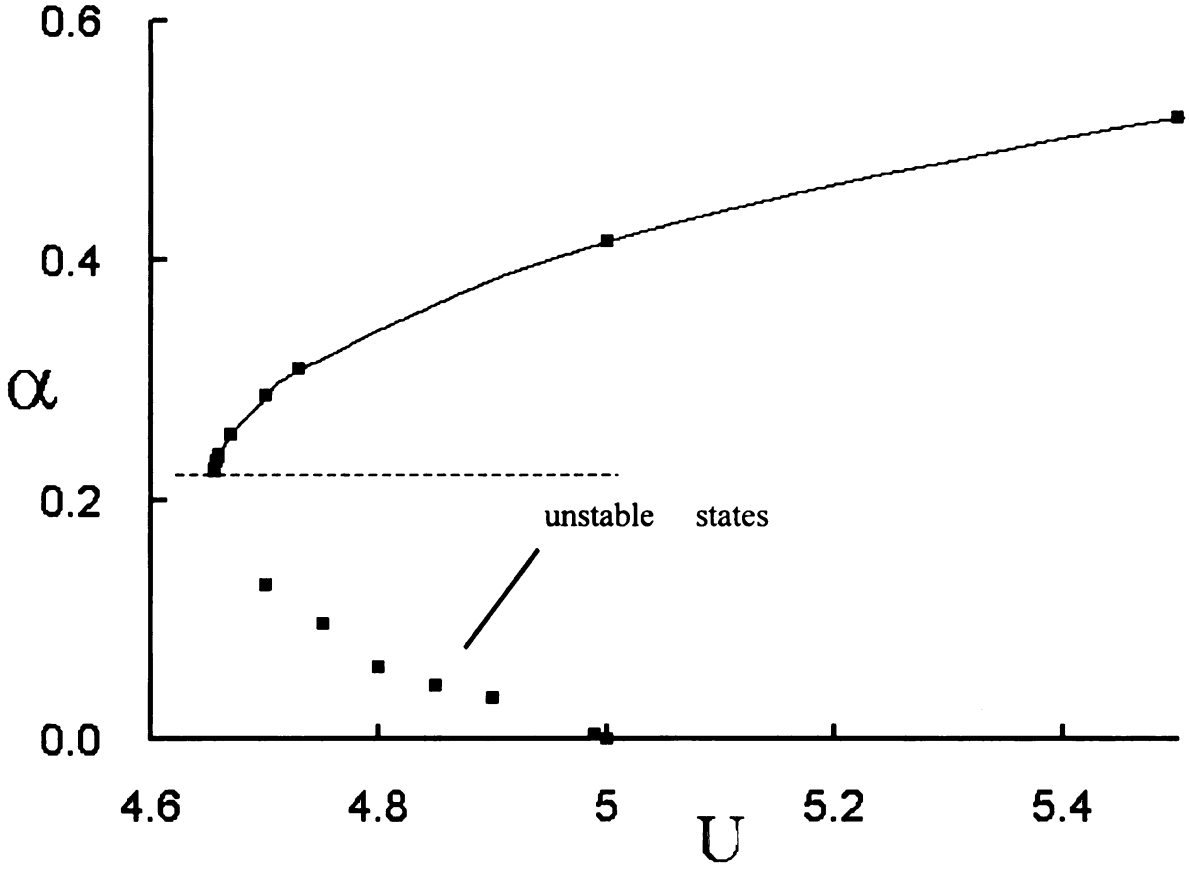

Figure 2.2 The isotropic-prolate transition predicted by the FSQ-closure for C_2=1/3 with the region between U_{ip} (5.0) and U_{pi} (4.626) enlarged

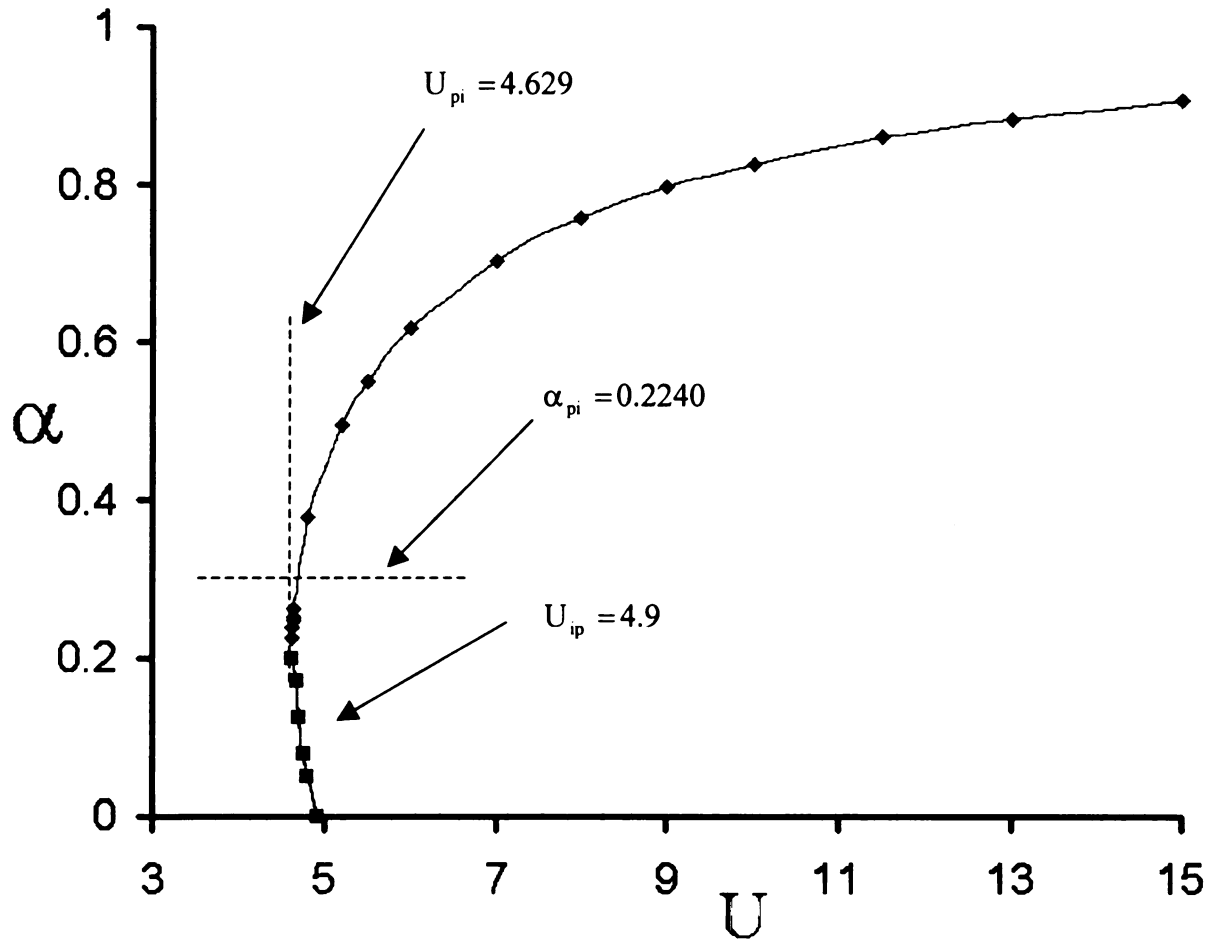

Figure 2.3 The isotropic-prolate transition predicted by the FSQ-closure with C_2=0.31. See Appendix F for the numerical values for the graph.

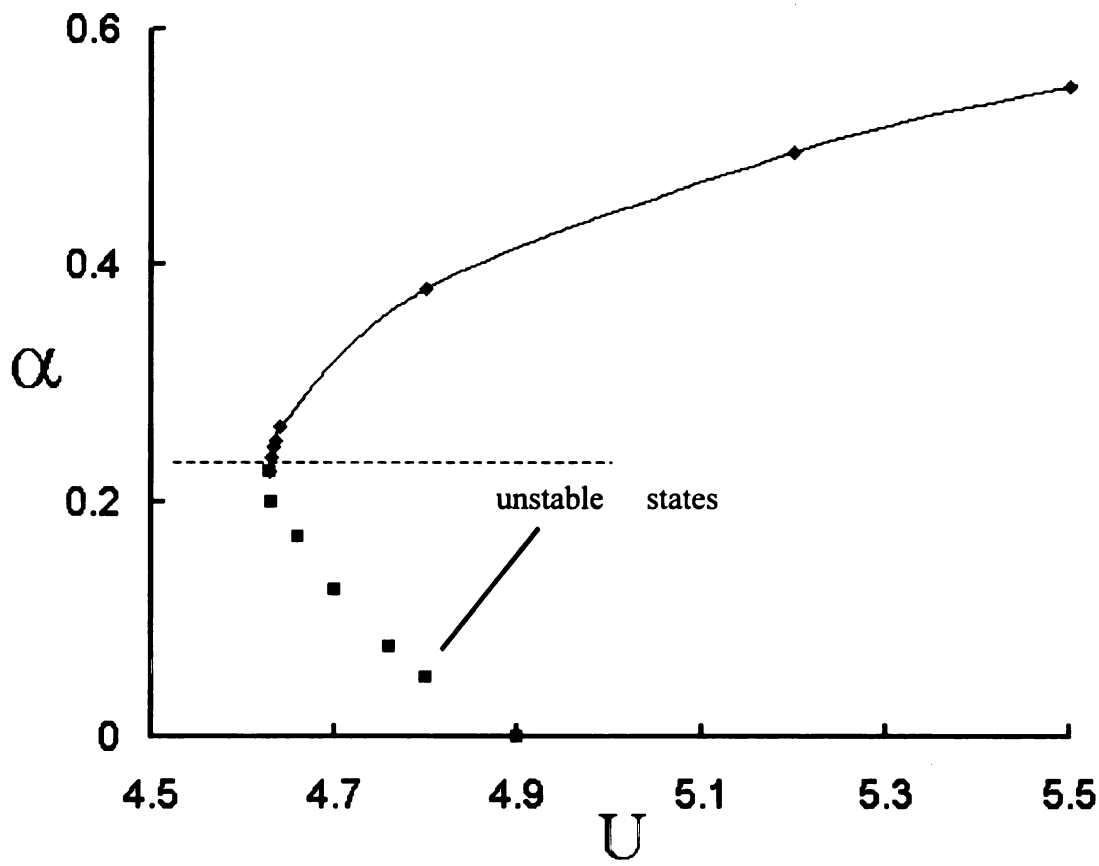

Figure 2.4 The isotropic-prolate transition predicted by the FSQ-closure for C_2=0.31 with the region between U_{ip} (4.9) and U_{pi} (4.629) enlarged

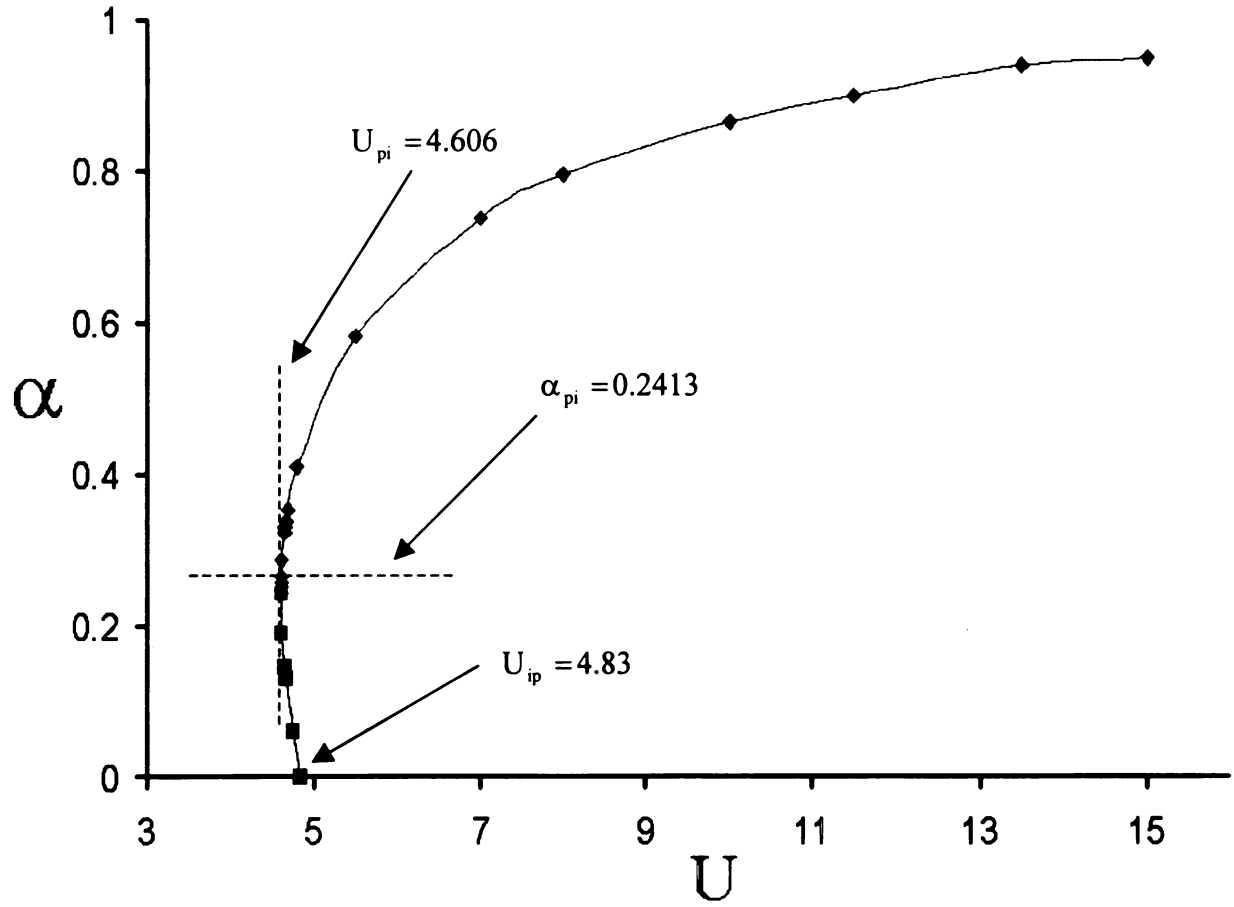

Figure 2.5 The isotropic-prolate transition predicted by the FSQ-closure with C_2=0.29.

See Appendix G for the numerical values for the graph.

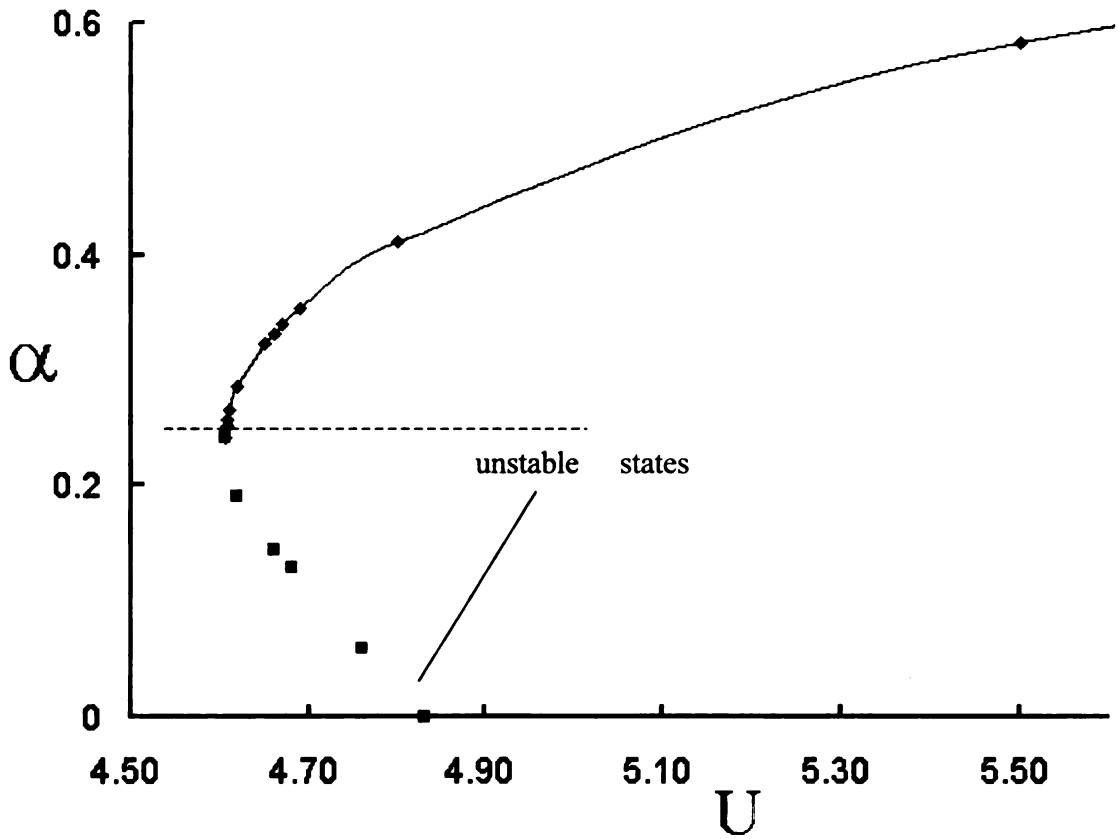

Figure 2.6 The isotropic-prolate transition predicted by the FSQ-closure for C_2=0.29 with the region between U_{ip} (4.83) and U_{pi} (4.606) enlarged.

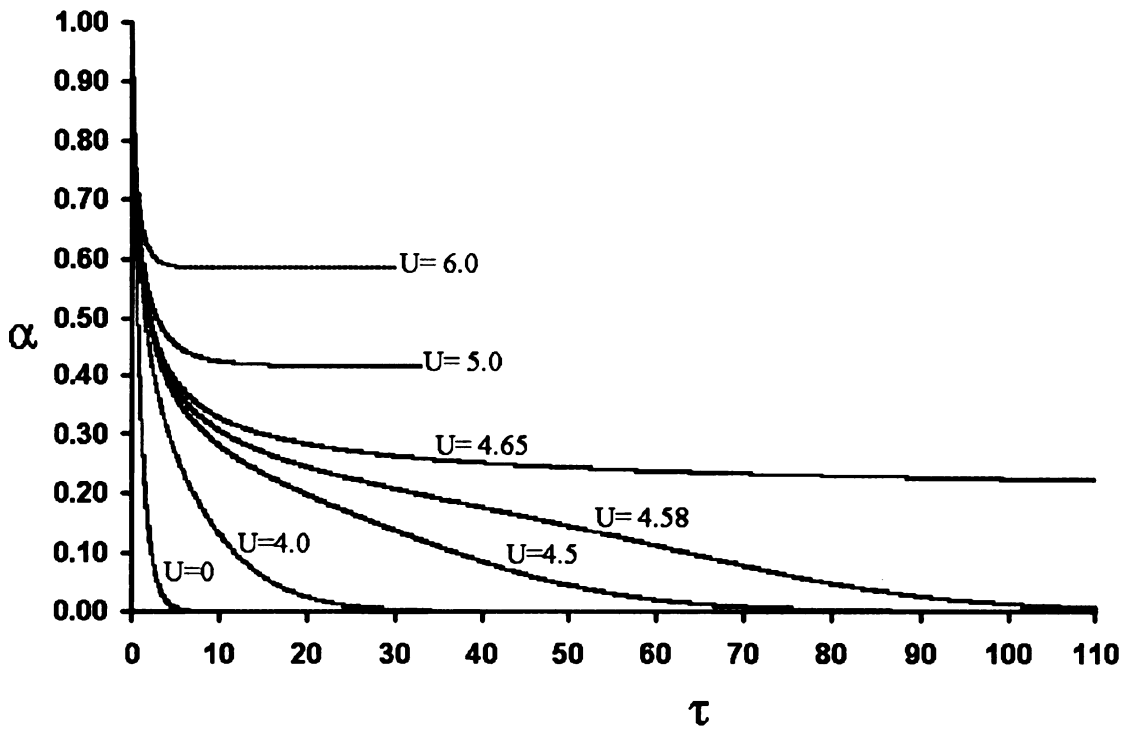

Figure 2.7 α versus τ (dimensionless time) for the relaxation of LCP microstructure from an initial nematic state with C_2=1/3.

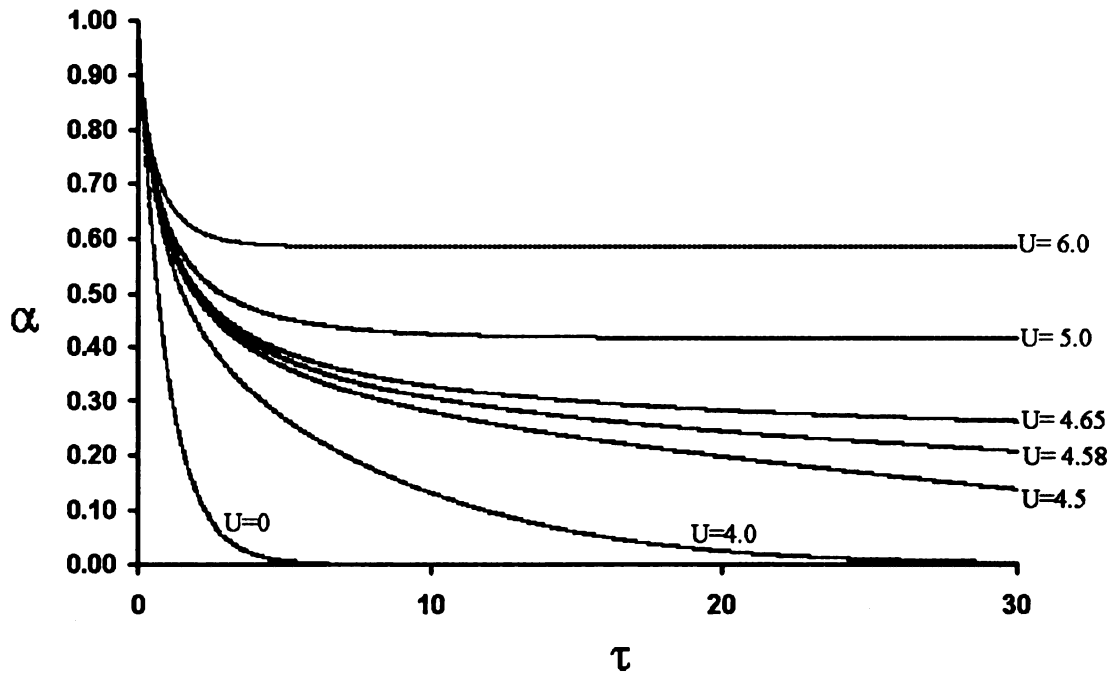

Figure 2.8 α versus τ (dimensionless time) for the relaxation of LCP microstructure from an initial nematic state with C_2= 1/3.

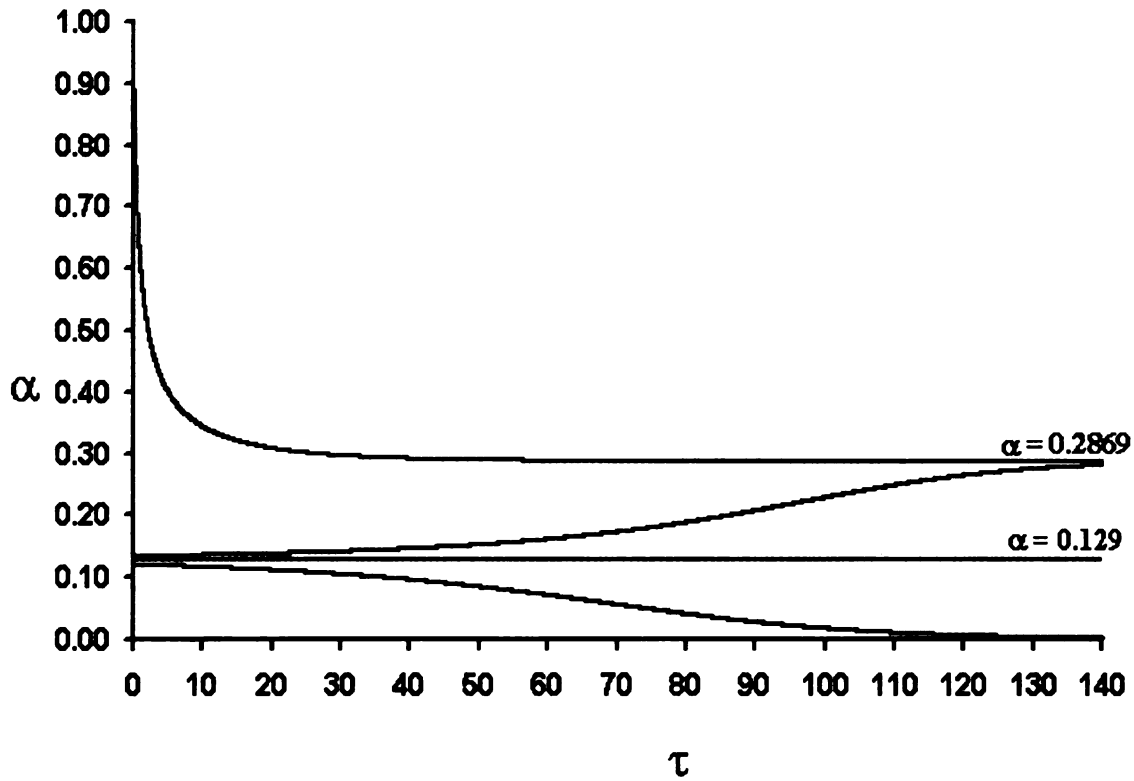

Figure 2.9 α versus τ (dimensionless time) for the relaxation of LCP microstructure from different initial states with C_2= 1/3 and U= 4.7.

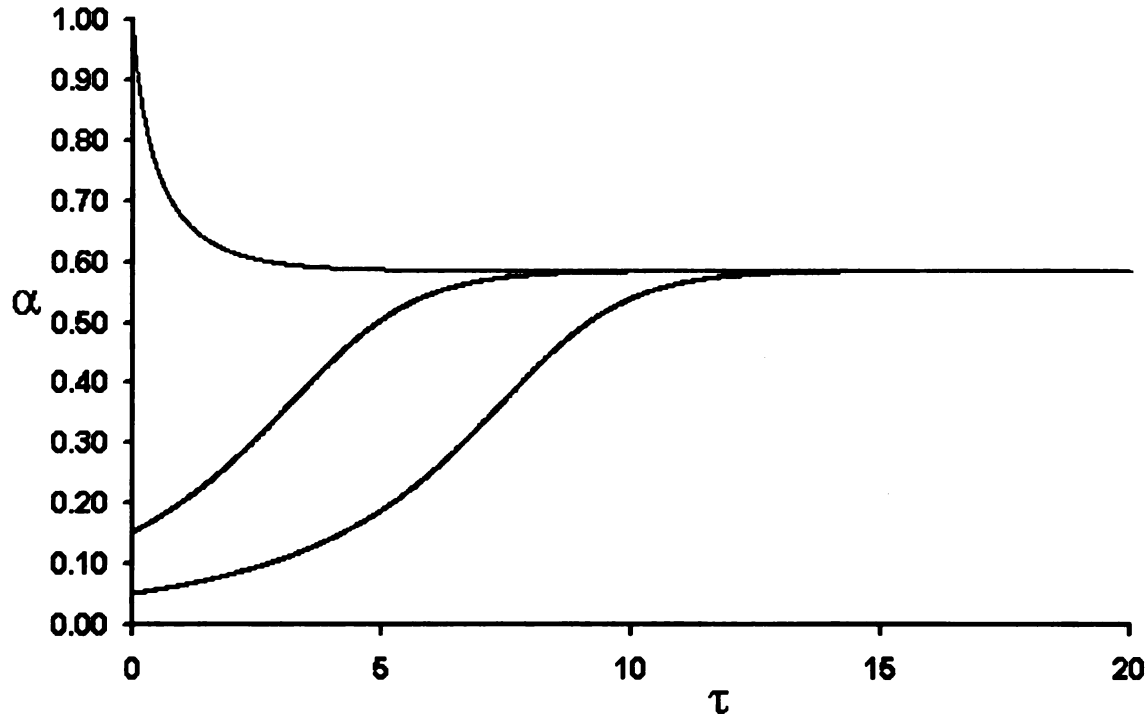

Figure 2.10 α versus τ (dimensionless time) for the relaxation of LCP microstructure from different initial states with C_2= 1/3 and U=6.

CHAPTER 3

CONCLUSIONS

Eq. (1.15) is solved using the FSQ-closure to evaluate the orientation tetradic, for different values of C_2 and U. By analyzing the results obtained, the following conclusion are made :

1.The U_{ip} =5.0 (see Kini *et al.* 2003) predicted by the FSQ-closure with C_2=1/3 is the same as that predicted by Chaubal *et al.*(1995) with the HL1 closure .

2. The values of U_{ip}, α_{pi}, U_{pi} predicted are dependent on the value of C_2 chosen. The region of transition (i.e., region between U_{ip} and U_{pi}) reduces as the value of C_2 decreases.

3. The magnitude of U relative to U_{ip} influences the relaxation times of the microstructure from an initial nematic state to an equilibrium state (see Chapter 2, Section 2.2).

4. The FSQ-closure exhibits the isotropic-prolate transition, qualitatively similar to those shown by the de-coupling approximation and the HL1 closure. A comparison of the U_{ip}, α_{pi}, U_{pi} for the de-coupling approximation, HL1 and FSQ-closures are listed in the Table 3.1. From Figure 3.1 it is evident that with C_2=1/3, the predictions made by FSQ-closure are closer to those made by the HL1 closure, and those with C_2=0.29 are closer to the predictions made by the de-coupling approximation closure.

3.1 Tables and Figures

Table 3.1 Comparison of the U_{ip}, U_{pi}, α_{pi}, values for the isotropic-prolate transition predicted by the FSQ-closure (C_2=1/3) with the HL1, and the de-coupling approximation.

Closure	U_{ip}	U_{pi}	α_{pi}	Reference
de-coupling approximation	3.00	2.667	0.2500	Bhave *et al.*1993
FSQ (C_2=1/3)	5.00	4.656	0.2258	This research
HL1	5.00	4.898	0.125	Chaubal *et al.*1995

Table 3.2 The U_{ip}, U_{pi}, α_{pi}, values for the isotropic-prolate transition predicted by the FSQ-closure with different C_2's.

C_2	U_{ip}	U_{pi}	α_{pi}
0.2900	4.83	4.606	0.2413
0.3100	4.90	4.629	0.2249
1/3	5.00	4.656	0.2258

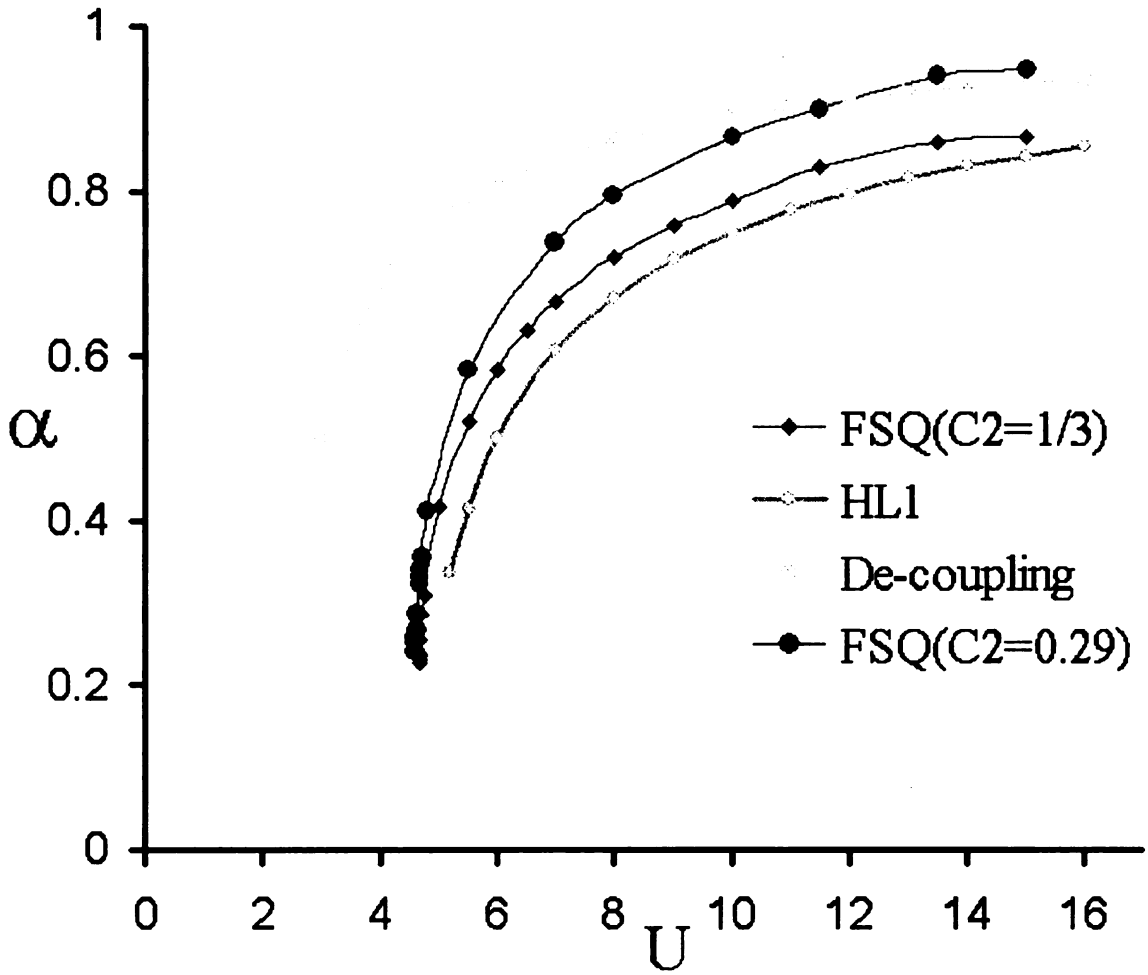

Figure 3.1 Comparison of the isotropic-prolate transition predicted by the FSQ-closure(C_2=1/3 and 0.29) with the HL1 and the de-coupling approximation.

CHAPTER 4

RECOMMENDATIONS

Experiments

The FSQ closure predicts an equilibrium phase diagram, which is qualitatively similar to those made by other closures like the HL1 and the de-coupling approximation. From Figure 3.1 it can be inferred that, the predictions made by the FSQ-closure are influenced by the particular value of C_2 chosen. These conclusions are based on the results of the theoretical results. Comparing these results with experimental data on the relaxation phenomena of lyotropic LCPs, will not only help in judging the predictions made by the FSQ-closure, but will also provides a basis for the selection of a C_2. The experimental data will also help in evaluating some of the underlying assumptions of the theory that D_R, the rotary diffusion coefficient and C_2 are constant.

Aharoni and Walsh (1979) observed the isotropic to anisotropic transition for liquid crystalline solutions of two, Poly (isocyanates). Beyond a critical concentration they observed that the solution separated into an isotropic and an anisotropic phase (liquid crystalline phase). The optical microscopy with cross-polarized light of the anisotropic phase showed that the isocyanate polymer was being aligned in a particular direction. Though these experiments were done with lyotropic LCPs that undergo phase separation, similar experimental studies with LCPs that do not phase separate should be able to determine the critical concentrations for phase transitions and provide experimental evidence for fixing a particular value for C_2.

The nematic strength U, is dependent on the number density of the molecules or the concentration of the molecules. So devising experiments to observe and characterize

the microstructure with different values of U, should yield an equilibrium phase diagram, which could then be compared with those deduced from theoretical models. Measuring the relaxation time for the limit of U=0, would provide an estimate of D_R the rotary diffusion co-efficient. The numerical results indicate that starting from an initial nematic state beyond U_{ip}, the equilibrium states all lie on the prolate line (see. Appendix .B). Characterizing the experimentally observed microstructure should help in understanding this theoretical observation.

Variation of C_2

For this research the values of C_2 used were 1/3, 0.31 and 0.29. Further simulations could be carried out with values of C_2 greater than 1/3.

APPENDIX A : INVARIANTS OF THE ORIENTATION DYADIC

The orientation dyadic $\underline{\underline{a}}=<\underline{p}\ \underline{p}>$ has three non-negative eigenvalues a_1, a_2, and a_3. Also associated with the tensor are the three invariants I_a, II_a and III_a.

$$I_a = \mathrm{tr}(\underline{\underline{a}}) = a_1 + a_2 + a_3 = 1 \tag{A.1}$$

$$II_a = \mathrm{tr}(\underline{\underline{a}} \cdot \underline{\underline{a}}) = (a_1)^2 + (a_2)^2 + (a_3)^2 \tag{A.2}$$

$$III_a = \mathrm{tr}(\underline{\underline{a}} \cdot \underline{\underline{a}} \cdot \underline{\underline{a}}) = (a_1)^3 + (a_2)^3 + (a_3)^3 \quad . \tag{A.3}$$

The structure tensor $\underline{\underline{b}}$ is defined as,

$$\underline{\underline{b}} = \underline{\underline{a}} - \underline{\underline{I}}/3 \quad . \tag{A.4}$$

Because $\underline{\underline{a}} = \underline{\underline{a}}^T$ and $\underline{\underline{I}} = \underline{\underline{I}}^T$ it follows that $\underline{\underline{b}} = \underline{\underline{b}}^T$.

Similarly, the invariants of $\underline{\underline{b}}$ can be written as

$$I_b = \mathrm{tr}(\underline{\underline{b}}) = b_1 + b_2 + b_3 = 0 \tag{A.5}$$

$$II_b = \mathrm{tr}(\underline{\underline{b}} \cdot \underline{\underline{b}}) = (b_1)^2 + (b_2)^2 + (b_3)^2 \tag{A.6}$$

$$III_b = \mathrm{tr}(\underline{\underline{b}} \cdot \underline{\underline{b}} \cdot \underline{\underline{b}}) = (b_1)^3 + (b_2)^3 + (b_3)^3 \quad . \tag{A.7}$$

where b_1, b_2, b_3 are the three eigenvalues of $\underline{\underline{b}}$.

The eigenvalues of $\underline{\underline{a}}$ and $\underline{\underline{b}}$ are related by

$$b_i = a_i - 1/3 \quad . \tag{A.8}$$

Therefore the nontrivial invariants of $\underline{\underline{b}}$ in terms of the eigenvalues of $\underline{\underline{a}}$ are given by

$$II_b = (a_1 - 1/3)^2 + (a_2 - 1/3)^2 + (a_3 - 1/3)^2 \tag{A.9}$$

$$III_b = (a_1 - 1/3)^3 + (a_2 - 1/3)^3 + (a_3 - 1/3)^3 \quad . \tag{A.10}$$

Figure A.1 Identifies the set of realizable orientation states (i.e., $0 \leq a_i \leq 1$).

Table A-1 defines the boundary of the invariant diagram (see Petty, *et al.* 1999; Nguyen, 2001;)

Table A-1. Invariants of the structure tensor

Orientation State	Invariants of $\underline{\underline{b}}$		Eigenvalues of $\langle \underline{p}\underline{p} \rangle$			
	II_b	III_b	1	2	3	Notes
A. Nematic	2/3	2/9	0	0	1	
B. Planar Anisotropic	$II_b=2/9 + 2\ III_b$		0	a	1-a	0< a<1/2
C. Smectic	1/6	-1/36	0	1/2	1/2	
D. Oblate	$II_b=6(-\ III_b/6)^{2/3}$		1-2a	a	a	1/3< a<1/2
E. Isotropic	0	0	1/3	1/3	1/3	
F. Prolate	$II_b=6(\ III_b/6)^{2/3}$		a	a	1-2a	0< a<1/3

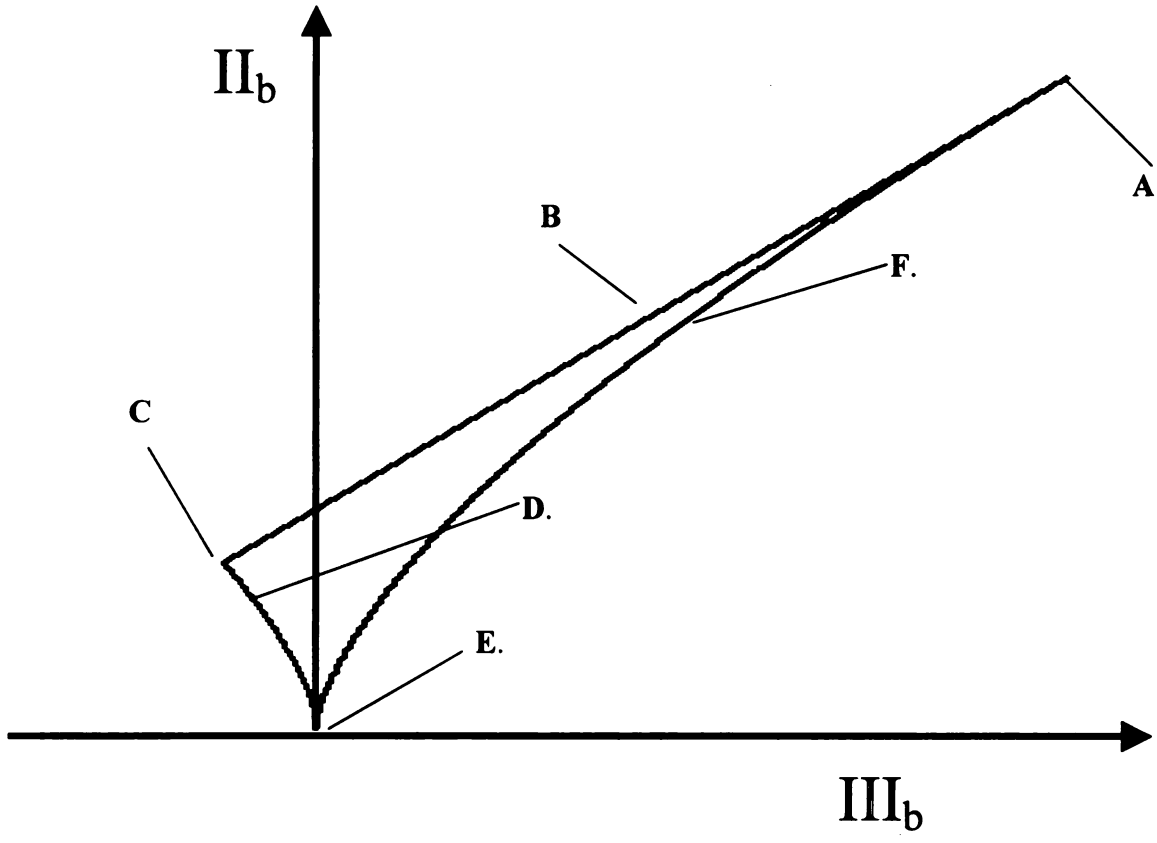

Figure A.1 Invariant diagram of the structure tensor $\underline{\underline{b}}$.

A. Nematic State

B. Planar Anisotropic States

C. Planar Isotropic State

D. Planar Axisymmetric

E. Isotropic States

F. Axial Axisymmetric

APPENDIX B : SCALAR ORDER PARAMETER FOR THE PROLATE STATES

The orientation order parameter α is a scalar measure of the orientation of the microstructure. α varies between the values 0 (isotropic) and 1 (nematic) and is defined by:

$$\alpha = \sqrt{(\frac{3}{2}\underline{\underline{b}}:\underline{\underline{b}})} \quad . \tag{B.1}$$

From Eq.(A.4), it follows that

$$\alpha = \sqrt{\frac{3}{2}(\underline{\underline{a}} - \frac{\underline{\underline{I}}}{3}):(\underline{\underline{a}} - \frac{\underline{\underline{I}}}{3})}$$

$$= \sqrt{\frac{3}{2}[\ \underline{\underline{a}}:\underline{\underline{a}} - \frac{2}{3} + \frac{1}{9}\underline{\underline{I}}:\underline{\underline{I}}\ ]}$$

$$= \sqrt{\frac{3}{2}[\ \underline{\underline{a}}:\underline{\underline{a}} - \frac{1}{3}\ ]}$$

$$\alpha = \sqrt{\frac{3}{2}(a_1^{\,2} + a_2^{\,2} + a_3^{\,2}) - \frac{1}{3}} \quad . \tag{B.2}$$

At the prolate states the three eigenvalues of $\underline{\underline{a}}$ are related as,

$$a_1 = a_2 \leq a_3$$

$$a_1 = a_2 = (1 - a_3)/2 \quad .$$

Therefore Eq. (B.2) can be written in terms of a_3 as follows

$$\alpha=\sqrt{\frac{3}{2}[2\left(\frac{1-a_3}{2}\right)^2+a_3{}^2-\frac{1}{3}]} \quad . \tag{B.3}$$

$$\alpha=\frac{3}{2}a_3-\frac{1}{2} \quad . \tag{B.4}$$

α=1 represents all the molecules perfectly aligned in one direction, while α=0 corresponds to an isotropic state.

APPENDIX C: TETRADIC CLOSURE AT THE NEMATIC STATE

C_2 is the coefficient corresponding to the quadratic term in the FSQ-closure.

The following calculations show that at the nematic state $C_2 = 1/3$.

At the nematic state

$$\langle \underline{\underline{pp}} \rangle = \underline{e}_3 \underline{e}_3$$

$$\langle \underline{\underline{ppp}}\underline{p} \rangle = \underline{e}_3 \underline{e}_3 \underline{e}_3 \underline{e}_3 .$$

$$\langle \underline{\underline{\underline{ppp}}}\underline{p} \rangle = (1-C_2)\langle \underline{\underline{\underline{ppp}}}\underline{p} \rangle_1 + C_2 \langle \underline{\underline{\underline{ppp}}}\underline{p} \rangle_2 . \tag{C.1}$$

$$\langle \underline{\underline{\underline{pppp}}} \rangle_1 \equiv -\frac{1}{35} S[\underline{\underline{\underline{I}}}\,\underline{\underline{I}}] + \frac{1}{7} S[\underline{\underline{I}} \langle \underline{\underline{pp}} \rangle] \tag{C.2}$$

$$\langle \underline{\underline{\underline{pppp}}} \rangle_2 = \frac{2}{35} \langle \underline{\underline{pp}} \rangle : \langle \underline{\underline{pp}} \rangle S[\underline{\underline{I}}\,\underline{\underline{I}}] + S[\langle \underline{\underline{pp}} \rangle \langle \underline{\underline{pp}} \rangle] - \frac{2}{7} S[\underline{\underline{I}} (\langle \underline{\underline{pp}} \rangle \cdot \langle \underline{\underline{pp}} \rangle)] ,$$

(C.3)

$$S[\underline{\underline{A}}, \underline{\underline{B}}] = A_{ij}B_{kl} + A_{ik}B_{jl} + A_{il}B_{jk} + A_{kl}B_{ij} + A_{ji}B_{ik} + A_{jk}B_{il} \tag{C.4}$$

The FSQ-closure at the nematic state reduces to,

$$\langle p_i p_j p_k p_l \rangle = -\frac{1}{35}(1-3C_2)(I_{ij}I_{kl} + I_{ik}I_{jl} + I_{il}I_{kj}) + \frac{1}{7}(1-3C_2)(I_{ij}\underline{e}_j\underline{e}_3 + I_{i3}\underline{e}_j\underline{e}_3 + I_{i3}\underline{e}_3\underline{e}_j + I_{kl}\underline{e}_3\underline{e}_3 + I_{3l}\underline{e}_3\underline{e}_k + I_{k3}\underline{e}_3\underline{e}_l) + 3C_2\underline{e}_3\underline{e}_3\underline{e}_3\underline{e}_3$$

(C.5)

Clearly $C_2 = 1/3$ yields the orientation state tetradic $\underline{e}_3\underline{e}_3\underline{e}_3\underline{e}_3$, which is representative of the nematic state

APPENDIX D: NUMERICAL DATA with C_2=1/3

The fourth order tetradic is computed with C_2=1/3 for the FSQ-closure and the differential equation Eq.(1.15) is solved for different values of U.

Table D.1 The eigenvalues of $\underline{\underline{a}}$, the structure parameter and the invariants of $\underline{\underline{b}}$ for U less than U_{pi} and with C_2=1/3

U	a_1	a_2	a_3	α	II_b	III_b
3.00	0.3333	0.3333	0.3334	0.0000	0.0000	0.0000
4.00	0.3333	0.3333	0.3334	0.0000	0.0000	0.0000
4.20	0.3333	0.3333	0.3334	0.0000	0.0000	0.0000
4.40	0.3333	0.3333	0.3334	0.0000	0.0000	0.0000

For $U < U_{pi}$, the microstructure relaxes to an isotropic state. The orientation dyadic is a diagonal matrix. Hence $a_{11}=a_1$, $a_{22}= a_2$ and $a_{33}= a_3$ .Where a_1, a_2 and a_3 are the eigenvalues of $\underline{\underline{a}}$. II_b, III_b are the second and third invariants of the anisotropic orientation tensor $\underline{\underline{b}}$. The isotropic state corresponds to point E on the invariant diagram (see Appendix A, Figure A-1).

Table D.2 The eigenvalues of $\underline{\underline{a}}$, the structure parameter α and the invariants of $\underline{\underline{b}}$ for U greater than U_{pi} and with $C_2=1/3$

U	a_1	a_2	a_3	α	II_b	III_b
4.659	0.2550	0.2550	0.4900	0.2350	0.0368	0.0029
4.660	0.2542	0.2542	0.4916	0.2374	0.0376	0.0030
4.700	0.2377	0.2377	0.5246	0.2869	0.0549	0.0052
4.730	0.2304	0.2304	0.5392	0.3088	0.0636	0.0065
5.000	0.1944	0.1944	0.6111	0.4167	0.1158	0.0161
5.500	0.1604	0.1604	0.6792	0.5188	0.1794	0.0310
6.000	0.1389	0.1389	0.7222	0.5833	0.2268	0.0441
6.500	0.1232	0.1232	0.7535	0.6303	0.2649	0.0556
7.000	0.1111	0.1111	0.7778	0.6667	0.2963	0.0659
8.000	0.0932	0.0932	0.8136	0.7204	0.3460	0.0831
9.000	0.0805	0.0805	0.8390	0.7585	0.3835	0.0970
10.000	0.0709	0.0709	0.8581	0.7872	0.4131	0.1084
11.500	0.0603	0.0603	0.8794	0.8191	0.4473	0.1221
13.500	0.0450	0.0450	0.9100	0.8650	0.4988	0.1438
15.000	0.0447	0.0447	0.9105	0.8658	0.4997	0.1442

For $U > U_{ip}$, the microstructure relaxes to a prolate state. The orientation dyadic is a diagonal matrix. The prolate states correspond to the line F on the invariant diagram (see Appendix A, Figure A-1). At the prolate state $a_{11} = a_{22} < a_{33}$.

Table D.3 The eigenvalues of $\underline{\underline{a}}$, the structure parameter and the invariants of $\underline{\underline{b}}$ for $U_{pi} \leq U \leq U_{ip}$ and with $C_2=1/3$.

U	a_1	a_2	a_3	α	II_b	III_b
4.70	0.2903	0.2903	0.4193	0.1290	0.0111	0.0005
4.75	0.3013	0.3013	0.3973	0.0960	0.0061	0.0002
4.80	0.3133	0.3133	0.3733	0.0600	0.0024	0.0000
4.85	0.3183	0.3183	0.3633	0.0450	0.0014	0.0000
4.90	0.3217	0.3217	0.3567	0.0350	0.0008	0.0000
5.00	0.3333	0.3333	0.3334	0.0001	0.0000	0.0000

The values of α tabulated correspond to the unstable states on Figure 2.2. These are the unstable states or the conditionally stable prolate states.

APPENDIX E: NUMERICAL DATA with C_2= 0.31

The fourth order tetradic is computed with C_2=0.31 for the FSQ-closure and Eq.(1.15) is solved for different values of U.

Table E.1 The eigenvalues of $\underline{\underline{a}}$, the structure parameter and the invariants of $\underline{\underline{b}}$ for U less than U_{pi} and with C_2=0.31

U	a_1	a_2	a_3	α	II_b	III_b
4.000	0.3333	0.3333	0.3334	0.0000	0.0000	0.0000
4.500	0.3333	0.3333	0.3334	0.0000	0.0000	0.0000
4.626	0.3333	0.3333	0.3334	0.0000	0.0000	0.0000
4.627	0.3333	0.3333	0.3334	0.0000	0.0000	0.0000

For $U < U_{pi}$, the microstructure relaxes to an isotropic state. The orientation dyadic is a diagonal matrix. Hence $a_{11}=a_1$, $a_{22}= a_2$ and $a_{33}= a_3$ .Where a_1, a_2 and a_3 are the eigenvalues of $\underline{\underline{a}}$. II_b, III_b are the second and third invariants of the anisotropic orientation tensor $\underline{\underline{b}}$. The isotropic state corresponds to point E on the invariant diagram (see Appendix A, Figure A-1).

Table E.2 The eigenvalues of $\underline{\underline{a}}$, the structure parameter and the invariants of $\underline{\underline{b}}$ for U greater than U_{pi} and with C_2=0.31

U	a_1	a_2	a_3	α	II_b	III_b
4.630	0.2561	0.2561	0.4877	0.2316	0.0358	0.0028
4.631	0.2539	0.2539	0.4922	0.2383	0.0379	0.0030
4.633	0.2512	0.2512	0.4975	0.2463	0.0404	0.0033
4.635	0.2493	0.2493	0.5014	0.2521	0.0424	0.0036
4.650	0.2405	0.2405	0.5190	0.2785	0.0517	0.0048
4.660	0.2365	0.2365	0.5270	0.2905	0.0563	0.0054
4.800	0.2070	0.2070	0.5861	0.3792	0.0958	0.0121
5.200	0.1678	0.1678	0.6644	0.4966	0.1644	0.0272
5.500	0.1495	0.1495	0.7010	0.5515	0.2028	0.0373
6.000	0.1275	0.1275	0.7449	0.6174	0.2541	0.0523
7.000	0.0990	0.0990	0.8020	0.7030	0.3295	0.0772
8.000	0.0806	0.0806	0.8388	0.7582	0.3832	0.0969
9.000	0.0675	0.0675	0.8650	0.7975	0.4240	0.1127
10.000	0.0576	0.0576	0.8848	0.8272	0.4562	0.1258
15.000	0.0305	0.0305	0.9389	0.9084	0.9389	0.9084

For $U > U_{ip}$, the microstructure relaxes to a prolate state. The orientation dyadic is a diagonal matrix. The prolate states correspond to the line F on the invariant diagram (see Appendix A, Figure A-1). At the prolate state $a_1 = a_2 < a_3$.

Table E.3 The eigenvalues of $\underline{\underline{a}}$, the structure parameter and the invariants of $\underline{\underline{b}}$ for $U_{pi} \leq U \leq U_{ip}$ and with C_2=0.31.

U	a_1	a_2	a_3	α	II_b	III_b
4.63	0.2667	0.2667	0.4667	0.2000	0.0267	0.0018
4.66	0.2767	0.2767	0.4467	0.1700	0.0193	0.0011
4.70	0.2917	0.2917	0.4167	0.1250	0.0104	0.0004
4.76	0.3077	0.3077	0.3847	0.0770	0.0040	0.0001
4.80	0.3167	0.3167	0.3667	0.0500	0.0017	0.0000
4.90	0.3333	0.3333	0.3334	0.0001	0.0000	0.0000

The values of α tabulated correspond to the unstable states on Figure 2.4. These are the unstable states or the conditionally stable prolate states.

APPENDIX F: NUMERICAL DATA with $C_2 = 0.29$

The fourth order tetradic is computed with C_2=0.29 for the FSQ-closure Eq.(1.15) is solved for different values of U.

Table F.1 The eigenvalues of $\underline{\underline{a}}$, the structure parameter and the invariants of $\underline{\underline{b}}$ for U less than U_{pi} and with C_2=0.29

U	a_1	a_2	a_3	α	II_b	III_b
2.500	0.3333	0.3333	0.3334	0.0000	0.0000	0.0000
3.500	0.3333	0.3333	0.3334	0.0000	0.0000	0.0000
4.200	0.3333	0.3333	0.3334	0.0000	0.0000	0.0000
4.600	0.3333	0.3333	0.3334	0.0000	0.0000	0.0000
4.605	0.3333	0.3333	0.3334	0.0000	0.0000	0.0000

For $U < U_{pi}$, the microstructure relaxes to an isotropic state. The orientation dyadic is a diagonal matrix. Hence $a_{11}=a_1$, $a_{22}= a_2$ and $a_{33}= a_3$ .Where a_1, a_2 and a_3 are the eigenvalues of $\underline{\underline{a}}$. II_b, III_b are the second and third invariants of the anisotropic orientation tensor $\underline{\underline{b}}$. The isotropic state corresponds to point E on the invariant diagram (see Appendix A, Figure A-1).

Table F.2 The eigenvalues of $\underline{\underline{a}}$, the structure parameter and the invariants of $\underline{\underline{b}}$ for U greater than U_{pi} and with C_2=0.29

U	a_1	a_2	a_3	α	II_b	III_b
4.607	0.2495	0.2495	0.5010	0.2515	0.0422	0.0035
4.608	0.2477	0.2477	0.5046	0.2569	0.0440	0.0038
4.610	0.2452	0.2452	0.5096	0.2644	0.0466	0.0041
4.620	0.2379	0.2379	0.5242	0.2863	0.0546	0.0052
4.650	0.2259	0.2259	0.5483	0.3225	0.0693	0.0075
4.660	0.2229	0.2229	0.5542	0.3313	0.0732	0.0081
4.670	0.2202	0.2202	0.5595	0.3393	0.0767	0.0087
4.690	0.2155	0.2155	0.5691	0.3537	0.0834	0.0098
4.800	0.1964	0.1964	0.6072	0.4108	0.1125	0.0154
5.500	0.1389	0.1389	0.7222	0.5833	0.2268	0.0441
7.000	0.0872	0.0872	0.8256	0.7384	0.3635	0.0895
8.000	0.0683	0.0683	0.8634	0.7951	0.4215	0.1117
10.000	0.0447	0.0447	0.9107	0.8661	0.5000	0.1444
11.500	0.0333	0.0333	0.9334	0.9001	0.5401	0.1621
13.500	0.0200	0.0200	0.9600	0.9400	0.5891	0.1846
15.000	0.0168	0.0168	0.9664	0.9496	0.6012	0.1903

For $U > U_{ip}$, the microstructure relaxes to a prolate state. The orientation dyadic is a diagonal matrix. The prolate states correspond to the line F on the invariant diagram (see Appendix A, Figure A-1). At the prolate state $a_1 = a_2 < a_3$.

Table F.3 The eigenvalues of $\underline{\underline{a}}$, the structure parameter and the invariants of $\underline{\underline{b}}$ for $U_{pi} \leq U \leq U_{ip}$ and with $C_2=0.29$

U	a_1	a_2	a_3	α	II_b	III_b
4.620	0.2700	0.2700	0.4600	0.1900	0.0241	0.0015
4.660	0.2850	0.2850	0.4300	0.1450	0.0140	0.0007
4.680	0.2900	0.2900	0.4200	0.1300	0.0113	0.0005
4.760	0.3133	0.3133	0.3733	0.0600	0.0024	0.0000
4.830	0.3333	0.3333	0.3334	0.0004	0.0000	0.0000

The values of α tabulated correspond to the unstable states on Figure 2.4. These are the unstable states or the conditionally stable prolate states

APPENDIX G: COMPUTER CODE (see. Nguyen, 2001)

The following is a Matlab code that solves the Eq. (1.15) by using a fourth-order Runge Kutta algorithm. The fourth order tetradic is computed using the FSQ-closure.

List of notations for computer code

Symbol	Definition	Corresponding notation used in the computer code
$\underline{\underline{a}} = \langle \underline{p}\underline{p} \rangle$	Orientation dyadic	a
$\langle \underline{p}\underline{p}\underline{p}\underline{p} \rangle$	Orientation tetradic	pppp0
$\underline{\underline{b}}$	Anisotropic orientation dyadic	b
II_b	Second invariant of $\underline{\underline{b}}$	IIb
III_b	Third invariant of $\underline{\underline{b}}$	IIIb
U	Nematic strength	U
τ	Dimensionless time	time
$\underline{\underline{I}}$	Identity matrix	ID
C_1	Coefficient of linear terms in FSQ-closure	C1
C_2	Coefficient of quadratic terms in FSQ-closure	C2
dt	step size	dt
stop	number of time steps	stop

Flow chart for computer code

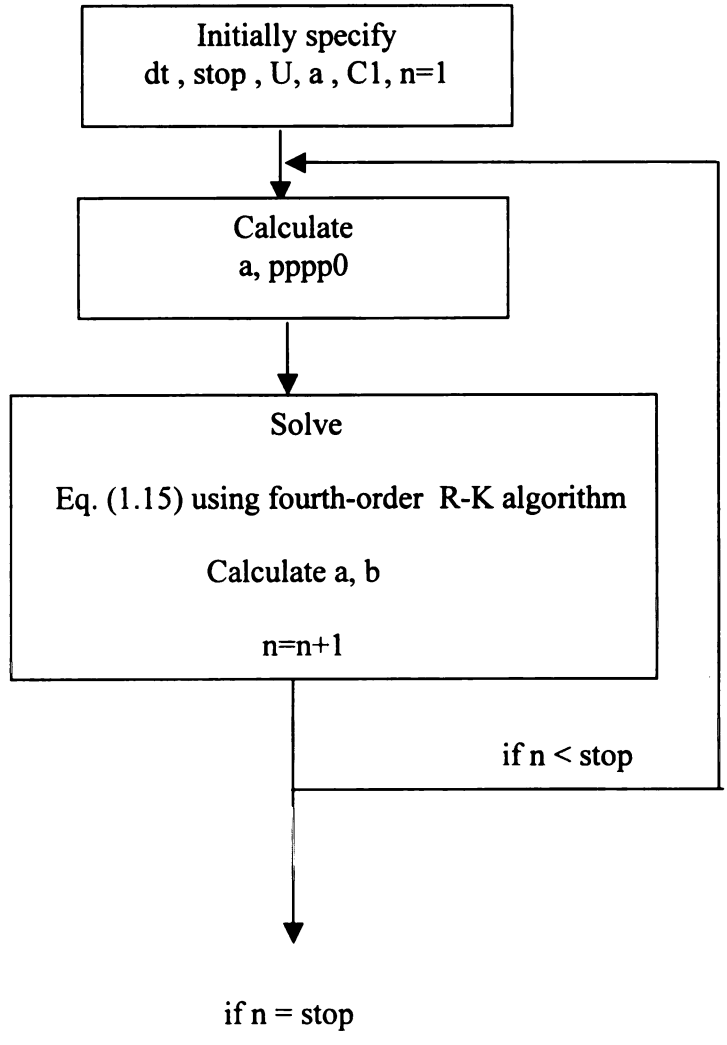

```
dt=0.01;
stop=90000;

%for liquid crystaline polymers;

lam=1.0;

U=4.626

C1=2/3;
C2=1-C1;

% %Initial input: perfect random;
a=[ 0     0     0
    0     0     0
    0     0     1 ] ;

%Unit tensor;
ID=[ 1 0 0
     0 1 0
     0 0 1 ];

s=0;

w=0;

%Defined parameter;
alpha=[ -1/35 1/7 0  0   0 0 0  0
        0  0  1 -2/7  0 0 0  0
        0  0  0 0   0 0 0  0
        0  0  0 0   0 0 1  -2/7 ] ;


%Symmetric and Antisymmetric portion of Velocity Gradient tensor;

for n=1:stop

  %First loop of the R-K method
  %Determine S[I I];
  for i=1:3
    for j=1:3
      for k=1:3
        for l=1:3
          SII(i,j,k,l)=ID(i,j)*ID(k,l)+ID(i,k)*ID(j,l)+ID(i,l)*ID(k,j);
        end
      end
```

```
    end
  end

  %Determine S[I a];
  for i=1:3
    for j=1:3
      for k=1:3
        for l=1:3
          SIa(i,j,k,l)=ID(i,j)*a(k,l)+ID(i,k)*a(j,l)+ID(i,l)*a(k,j);
          SIa(i,j,k,l)=a(i,j)*ID(k,l)+a(i,k)*ID(j,l)+a(i,l)*ID(k,j)+SIa(i,j,k,l);
        end
      end
    end
  end


%Determine S[a a];
  for i=1:3
    for j=1:3
      for k=1:3
        for l=1:3
          Saa(i,j,k,l)=a(i,j)*a(k,l)+a(i,k)*a(j,l)+a(i,l)*a(k,j);
        end
      end
    end
  end

  %Determine S[I(a*a)];
  for i=1:3
    for j=1:3
      aa(i,j)=0;
      bb(i,j)=0;
      for k=1:3
        aa(i,j) = aa(i,j)+a(i,k)*a(k,j);
        bb(i,j) = bb(i,j)+(a(i,k)-ID(i,k)/3)*(a(k,j)-ID(k,j)/3);
      end
    end
  end

  for i=1:3
    for j=1:3
      for k=1:3
        for l=1:3
          SIaa(i,j,k,l)=ID(i,j)*aa(k,l)+ID(i,k)*aa(j,l)+ID(i,l)*aa(k,j);
          SIaa(i,j,k,l)=aa(i,j)*ID(k,l)+aa(i,k)*ID(j,l)+aa(i,l)*ID(k,j)+SIaa(i,j,k,l);
        end
```

```
      end
    end
  end

  %Determine S[(a*a)a];
  for i=1:3
    for j=1:3
      aa(i,j)=0;
      for k=1:3
        aa(i,j)=aa(i,j)+a(i,k)*a(k,j);
      end
    end
  end

for i=1:3
    for j=1:3
      for k=1:3
        for l=1:3
          Saaa(i,j,k,l)=aa(i,j)*a(k,l)+aa(i,k)*a(j,l)+aa(i,l)*a(k,j);
          Saaa(i,j,k,l)=a(i,j)*aa(k,l)+a(i,k)*aa(j,l)+a(i,l)*aa(k,j)+Saaa(i,j,k,l);
        end
      end
    end
  end

  %Determine SIaaa;
  for i=1:3
    for j=1:3
      aaa(i,j)=0;
      bbb(i,j)=0;
      for k=1:3
        aaa(i,j)=aaa(i,j)+aa(i,k)*a(k,j);
        bbb(i,j)=bbb(i,j)+bb(i,k)*(a(k,j)-ID(k,j)/3);
      end
    end
  end


  for i=1:3
    for j=1:3
      for k=1:3
        for l=1:3
          SIaaa(i,j,k,l)=ID(i,j)*aaa(k,l)+ID(i,k)*aaa(j,l)+ID(i,l)*aaa(k,j);
          SIaaa(i,j,k,l) = aaa(i,j)*ID(k,l)+aaa(i,k)*ID(j,l)+aaa(i,l)*ID(k,j)+SIaaa(i,j,k,l);
        end
      end
```

```
    end
  end

  %Determine S[(a*a)(a*a)];
  for i=1:3
    for j=1:3
      for k=1:3
        for l=1:3
          Saaaa(i,j,k,l)=aa(i,j)*aa(k,l)+aa(i,k)*aa(j,l)+aa(i,l)*aa(k,j);
        end
      end
    end
  end



%Determine S[I(a*a*a*a)];
  for i =1:3
    for j=1:3
      aaaa(i,j)=0;
      for k=1:3
        aaaa(i,j)=aaaa(i,j)+aaa(i,k)*a(k,j);
      end
    end
  end

  for i=1:3
    for j=1:3
      for k=1:3
        for l=1:3
          SIaaaa(i,j,k,l)=ID(i,j)*aaaa(k,l)+ID(i,k)*aaaa(j,l)+ID(i,l)*aaaa(k,j);

SIaaaa(i,j,k,l)=aaaa(i,j)*ID(k,l)+aaaa(i,k)*ID(j,l)+aaaa(i,l)*ID(k,j)+SIaaaa(i,j,k,l);
        end
      end
    end
  end

  %Determine a:a (IIa) and alpha(2,1);
  IIa=aa(1,1)+aa(2,2)+aa(3,3);
  IIb=bb(1,1)+bb(2,2)+bb(3,3);
  alpha(2,1)=2*IIa/35;

  %Determine alpha(3,1);
  ALP1=aaa(1,1)+aaa(2,2)+aaa(3,3);
  alpha(3,1)=1/35+(4/35)*(ALP1/IIa);
```

```
IIIa=aaa(1,1)+aaa(2,2)+aaa(3,3);
IIIb=bbb(1,1)+bbb(2,2)+bbb(3,3);

%Determine alpha(3,4);
alpha(3,4)=-1/(7*IIa);

%Determine alpha(3,5);
alpha(3,5)=1/IIa;

%Determine alpha(3,6);
alpha(3,6)=-4/(7*IIa);

%Determine alpha(4,1);
ALP2=aaaa(1,1)+aaaa(2,2)+aaaa(3,3);
alpha(4,1)=2/35*ALP2+(1/35)*IIa*IIa;

%Determine alpha(4,4);
alpha(4,4)=(-1/7)*IIa;


%MSU contribution;
%Determine pppp1,pppp2
 for i=1:3
  for j=1:3
    for k=1:3
      for l=1:3
        pppp5(i,j,k,l)=a(i,j)*a(k,l);
        pppp1(i,j,k,l)=alpha(1,1)*SII(i,j,k,l)+alpha(1,2)*SIa(i,j,k,l);

%pppp2(i,j,k,l)=alpha(2,1)*SII(i,j,k,l)+alpha(2,2)*SIa(i,j,k,l)+alpha(2,3)*Saa(i,j,k,l)+alp
ha(2,4)*SIaa(i,j,k,l);

pppp2(i,j,k,l)=alpha(2,1)*SII(i,j,k,l)+alpha(2,3)*Saa(i,j,k,l)+alpha(2,4)*SIaa(i,j,k,l);


        %Case1:Michigan State University model;
        pppp0(i,j,k,l)=C1*pppp1(i,j,k,l)+C2*pppp2(i,j,k,l);

      end
    end
  end
end

%Determine <pppp>:S
for i=1:3
  for j=1:3
```

```
      M(i,j)=0;
      for k=1:3
        for l=1:3
          M(i,j)=M(i,j)+pppp0(i,j,k,l)*s(l,k);
        end
      end
    end
  end

  %Determine <pp>:<pppp>
  for i=1:3
    for j=1:3
      N(i,j)=0;
      for k=1:3
        for l=1:3
          N(i,j)=N(i,j)+pppp0(i,j,k,l)*a(l,k);
        end
      end
    end
  end

  %Determine S.a+a.S, W.a+a.W(T);
  for i=1:3
    for j=1:3
      saas(i,j)=0;
      waaw(i,j)=0;
      for k=1:3
        saas(i,j)=saas(i,j)+s(i,k)*a(k,j)+a(i,k)*s(k,j);
        waaw(i,j)=waaw(i,j)+w(i,k)*a(k,j)+a(i,k)*w(j,k);
      end
    end
  end

  %Right handside of the equation
  for i=1:3
    for j=1:3
      dk1(i,j)=(ID(i,j)/3-a(i,j))+lam*Pe*(saas(i,j)-2*M(i,j))-Pe*waaw(i,j)+U*(aa(i,j)-
N(i,j));
    end
  end

  %2nd loop of 4th order R_K

  for i=1:3
    for j=1:3
      a1(i,j)=a(i,j)+dk1(i,j)*dt*0.5;
```

```
  end
end

%Determine S[I a];
for i=1:3
  for j=1:3
    for k=1:3
      for l=1:3
        SIa1(i,j,k,l)=ID(i,j)*a1(k,l)+ID(i,k)*a1(j,l)+ID(i,l)*a1(k,j);
        SIa1(i,j,k,l)=a1(i,j)*ID(k,l)+a1(i,k)*ID(j,l)+a1(i,l)*ID(k,j)+SIa1(i,j,k,l);
      end
    end
  end
end

%Determine S[a a];
for i=1:3
  for j=1:3
    for k=1:3
      for l=1:3
        Saa1(i,j,k,l)=a1(i,j)*a1(k,l)+a1(i,k)*a1(j,l)+a1(i,l)*a1(k,j);
      end
    end
  end
end

%Determine S[I(a*a)];
for i=1:3
  for j=1:3
    aa1(i,j)=0;
    bb1(i,j)=0;
    for k=1:3
      aa1(i,j) = aa1(i,j)+a1(i,k)*a1(k,j);
      bb1(i,j) = bb1(i,j)+(a1(i,k)-ID(i,k)/3)*(a1(k,j)-ID(k,j)/3);
    end
  end
end

for i=1:3
  for j=1:3
    for k=1:3
      for l=1:3
        SIaa1(i,j,k,l)=ID(i,j)*aa1(k,l)+ID(i,k)*aa1(j,l)+ID(i,l)*aa1(k,j);
        SIaa1(i,j,k,l)=aa1(i,j)*ID(k,l)+aa1(i,k)*ID(j,l)+aa1(i,l)*ID(k,j)+SIaa1(i,j,k,l);
      end
    end
```

```
    end
  end

  %Determine S[(a*a)a];
  for i=1:3
    for j=1:3
      aa1(i,j)=0;
      for k=1:3
        aa1(i,j)=aa1(i,j)+a1(i,k)*a1(k,j);
      end
    end
  end

  for i=1:3
    for j=1:3
      for k=1:3
        for l=1:3
          Saaa1(i,j,k,l)=aa1(i,j)*a1(k,l)+aa1(i,k)*a1(j,l)+aa1(i,l)*a1(k,j);
          Saaa1(i,j,k,l)=a1(i,j)*aa1(k,l)+a1(i,k)*aa1(j,l)+a1(i,l)*aa1(k,j)+Saaa1(i,j,k,l);
        end
      end
    end
  end

  %Determine SIaaa;
  for i=1:3
    for j=1:3
      aaa1(i,j)=0;
      bbb1(i,j)=0;
      for k=1:3
        aaa1(i,j)=aaa1(i,j)+aa1(i,k)*a1(k,j);
        bbb1(i,j)=bbb1(i,j)+bb1(i,k)*(a1(k,j)-ID(k,j)/3);
      end
    end
  end


  for i=1:3
    for j=1:3
      for k=1:3
        for l=1:3
          SIaaa1(i,j,k,l)=ID(i,j)*aaa1(k,l)+ID(i,k)*aaa1(j,l)+ID(i,l)*aaa1(k,j);
          SIaaa1(i,j,k,l) =
aaa1(i,j)*ID(k,l)+aaa1(i,k)*ID(j,l)+aaa1(i,l)*ID(k,j)+SIaaa1(i,j,k,l);
        end
      end
```

```
    end
  end

  %Determine S[(a*a)(a*a)];
  for i=1:3
    for j=1:3
      for k=1:3
        for l=1:3
          Saaaa1(i,j,k,l)=aa1(i,j)*aa1(k,l)+aa1(i,k)*aa1(j,l)+aa1(i,l)*aa1(k,j);
        end
      end
    end
  end

 %Determine S[I(a*a*a*a)];
  for i =1:3
    for j=1:3
      aaaa1(i,j)=0;
      for k=1:3
        aaaa1(i,j)=aaaa1(i,j)+aaa1(i,k)*a1(k,j);
      end
    end
  end

  for i=1:3
    for j=1:3
      for k=1:3
        for l=1:3
          SIaaaa1(i,j,k,l)=ID(i,j)*aaaa1(k,l)+ID(i,k)*aaaa1(j,l)+ID(i,l)*aaaa1(k,j);

SIaaaa1(i,j,k,l)=aaaa1(i,j)*ID(k,l)+aaaa1(i,k)*ID(j,l)+aaaa1(i,l)*ID(k,j)+SIaaaa1(i,j,k,l);
        end
      end
    end
  end
  %Determine a:a (IIa) and alpha(2,1);
  IIa1=aa1(1,1)+aa1(2,2)+aa1(3,3);
  IIb1=bb1(1,1)+bb1(2,2)+bb1(3,3);
  alpha1(2,1)=2*(IIa1)/35;

  %Determine alpha(3,1);
  ALP11=aaa1(1,1)+aaa1(2,2)+aaa1(3,3);
  alpha1(3,1)=1/35+(4/35)*(ALP11/IIa1);
  IIIa1=aaa1(1,1)+aaa1(2,2)+aaa1(3,3);
  IIIb1=bbb1(1,1)+bbb1(2,2)+bbb1(3,3);
```

```
%Determine alpha(3,4);
alpha1(3,4)=1/(7*IIa1);

%Determine alpha(3,5);
alpha1(3,5)=1/IIa1;

%Determine alpha(3,6);
alpha1(3,6)=-4/(7*IIa1);

%Determine alpha(4,1);
ALP21=aaaa1(1,1)+aaaa1(2,2)+aaaa1(3,3);
alpha1(4,1)=2/35*ALP21+(1/35)*IIa1*IIa1;

%Determine alpha(4,4);
alpha1(4,4)=(-1/7)*IIa1;


%MSU contribution;
%Determine pppp1,pppp2,pppp3,pppp4;
for i=1:3
  for j=1:3
    for k=1:3
      for l=1:3
        pppp51(i,j,k,l)=a1(i,j)*a1(k,l);
        pppp11(i,j,k,l)=alpha(1,1)*SII(i,j,k,l)+alpha(1,2)*SIa1(i,j,k,l);

%pppp2(i,j,k,l)=alpha(2,1)*SII(i,j,k,l)+alpha(2,2)*SIa(i,j,k,l)+alpha(2,3)*Saa(i,j,k,l)+alp
ha(2,4)*SIaa(i,j,k,l);

pppp21(i,j,k,l)=alpha1(2,1)*SII(i,j,k,l)+alpha(2,3)*Saa1(i,j,k,l)+alpha(2,4)*SIaa1(i,j,k,l);

        %Case1:Michigan State University model;
        pppp01(i,j,k,l)=C1*pppp11(i,j,k,l)+C2*pppp21(i,j,k,l);
      end
    end
  end
end

%Determine <pppp>:S
for i=1:3
  for j=1:3
    M1(i,j)=0;
    for k=1:3
      for l=1:3
        M1(i,j)=M1(i,j)+pppp01(i,j,k,l)*s(l,k);
      end
```

```
    end
  end
end

%Determine <pp>:<pppp>
for i=1:3
  for j=1:3
    N1(i,j)=0;
    for k=1:3
      for l=1:3
        N1(i,j)=N1(i,j)+pppp01(i,j,k,l)*a1(l,k);
      end
    end
  end
end

%Determine S.a+a.S, W.a+a.W(T);
for i=1:3
  for j=1:3
    saas1(i,j)=0;
    waaw1(i,j)=0;
    for k=1:3
      saas1(i,j)=saas1(i,j)+s(i,k)*a1(k,j)+a1(i,k)*s(k,j);
      waaw1(i,j)=waaw1(i,j)+w(i,k)*a1(k,j)+a1(i,k)*w(j,k);
    end
  end
end


%Right handside of the equation
for i=1:3
  for j=1:3
    dk2(i,j)=(ID(i,j)/3-a1(i,j))+lam*Pe*(saas1(i,j)-2*M1(i,j))-
Pe*waaw1(i,j)+U*(aa1(i,j)-N1(i,j));
  end
end

%3rd loop of 4th order R-K

for i=1:3
  for j=1:3
    a2(i,j)=a(i,j)+dk2(i,j)*dt*0.5;
  end
end

%Determine S[I a];
```

```
  for i=1:3
    for j=1:3
      for k=1:3
        for l=1:3
          SIa2(i,j,k,l)=ID(i,j)*a2(k,l)+ID(i,k)*a2(j,l)+ID(i,l)*a2(k,j);
          SIa2(i,j,k,l)=a2(i,j)*ID(k,l)+a2(i,k)*ID(j,l)+a2(i,l)*ID(k,j)+SIa2(i,j,k,l);
        end
      end
    end
  end

%Determine S[a a];
  for i=1:3
    for j=1:3
      for k=1:3
        for l=1:3
          Saa2(i,j,k,l)=a2(i,j)*a2(k,l)+a2(i,k)*a2(j,l)+a2(i,l)*a2(k,j);
        end
      end
    end
  end

  %Determine S[I(a*a)];
  for i=1:3
    for j=1:3
      aa2(i,j)=0;
      bb2(i,j)=0;
      for k=1:3
        aa2(i,j) = aa2(i,j)+a2(i,k)*a2(k,j);
        bb2(i,j) = bb2(i,j)+(a2(i,k)-ID(i,k)/3)*(a2(k,j)-ID(k,j)/3);
      end
    end
  end

  for i=1:3
    for j=1:3
      for k=1:3
        for l=1:3
          SIaa2(i,j,k,l)=ID(i,j)*aa2(k,l)+ID(i,k)*aa2(j,l)+ID(i,l)*aa2(k,j);
          SIaa2(i,j,k,l)=aa2(i,j)*ID(k,l)+aa2(i,k)*ID(j,l)+aa2(i,l)*ID(k,j)+SIaa2(i,j,k,l);
        end
      end
    end
  end

  %Determine S[(a*a)a];
```

```
for i=1:3
  for j=1:3
    aa2(i,j)=0;
    for k=1:3
      aa2(i,j)=aa2(i,j)+a2(i,k)*a2(k,j);
    end
  end
end

 for i=1:3
  for j=1:3
    for k=1:3
      for l=1:3
        Saaa2(i,j,k,l)=aa2(i,j)*a2(k,l)+aa2(i,k)*a2(j,l)+aa2(i,l)*a2(k,j);
        Saaa2(i,j,k,l)=a2(i,j)*aa2(k,l)+a2(i,k)*aa2(j,l)+a2(i,l)*aa2(k,j)+Saaa2(i,j,k,l);
      end
    end
  end
end

%Determine SIaaa;
for i=1:3
  for j=1:3
    aaa2(i,j)=0;
    bbb2(i,j)=0;
    for k=1:3
      aaa2(i,j)=aaa2(i,j)+aa2(i,k)*a2(k,j);
      bbb2(i,j)=bbb2(i,j)+bb2(i,k)*(a2(k,j)-ID(k,j)/3);
    end
  end
end


for i=1:3
  for j=1:3
    for k=1:3
      for l=1:3
        SIaaa2(i,j,k,l)=ID(i,j)*aaa2(k,l)+ID(i,k)*aaa2(j,l)+ID(i,l)*aaa2(k,j);
        SIaaa2(i,j,k,l) =
aaa2(i,j)*ID(k,l)+aaa2(i,k)*ID(j,l)+aaa2(i,l)*ID(k,j)+SIaaa2(i,j,k,l);
      end
    end
  end
end

%Determine S[(a*a)(a*a)];
```

```
  for i=1:3
    for j=1:3
      for k=1:3
        for l=1:3
          Saaaa2(i,j,k,l)=aa2(i,j)*aa2(k,l)+aa2(i,k)*aa2(j,l)+aa2(i,l)*aa2(k,j);
        end
      end
    end
  end


%Determine S[I(a*a*a*a)];
  for i =1:3
    for j=1:3
      aaaa2(i,j)=0;
      for k=1:3
        aaaa2(i,j)=aaaa2(i,j)+aaa2(i,k)*a2(k,j);
      end
    end
  end

  for i=1:3
    for j=1:3
      for k=1:3
        for l=1:3
          SIaaaa2(i,j,k,l)=ID(i,j)*aaaa2(k,l)+ID(i,k)*aaaa2(j,l)+ID(i,l)*aaaa2(k,j);

SIaaaa2(i,j,k,l)=aaaa2(i,j)*ID(k,l)+aaaa2(i,k)*ID(j,l)+aaaa2(i,l)*ID(k,j)+SIaaaa2(i,j,k,l);
        end
      end
    end
  end
  %Determine a:a (IIa) and alpha(2,1);
  IIa2=aa2(1,1)+aa2(2,2)+aa2(3,3);
  IIb2=bb2(1,1)+bb2(2,2)+bb2(3,3);
  alpha2(2,1)=2*(IIa2)/35;

  %Determine alpha(3,1);
  ALP12=aaa2(1,1)+aaa2(2,2)+aaa2(3,3);
  alpha2(3,1)=1/35+(4/35)*(ALP12/IIa2);
  IIIa2=aaa2(1,1)+aaa2(2,2)+aaa2(3,3);
  IIIb2=bbb2(1,1)+bbb2(2,2)+bbb2(3,3);

  %Determine alpha(3,4);
  alpha2(3,4)=1/(7*IIa2);
```

```
  %Determine alpha(3,5);
  alpha2(3,5)=1/IIa2;

  %Determine alpha(3,6);
  alpha2(3,6)=-4/(7*IIa2);

  %Determine alpha(4,1);
  ALP22=aaaa2(1,1)+aaaa2(2,2)+aaaa2(3,3);
  alpha2(4,1)=2/35*ALP22+(1/35)*IIa2*IIa2;

  %Determine alpha(4,4);
  alpha2(4,4)=(-1/7)*IIa2;



%MSU contribution;
  %Determine pppp1
  for i=1:3
    for j=1:3
      for k=1:3
        for l=1:3
          pppp52(i,j,k,l)=a2(i,j)*a2(k,l);
          pppp12(i,j,k,l)=alpha(1,1)*SII(i,j,k,l)+alpha(1,2)*SIa2(i,j,k,l);

%pppp2(i,j,k,l)=alpha(2,1)*SII(i,j,k,l)+alpha(2,2)*SIa(i,j,k,l)+alpha(2,3)*Saa(i,j,k,l)+alp
ha(2,4)*SIaa(i,j,k,l);

pppp22(i,j,k,l)=alpha2(2,1)*SII(i,j,k,l)+alpha(2,3)*Saa2(i,j,k,l)+alpha(2,4)*SIaa2(i,j,k,l);

pppp32(i,j,k,l)=alpha2(3,1)*SII(i,j,k,l)+alpha2(3,4)*SIaa2(i,j,k,l)+alpha2(3,5)*Saaa2(i,j,k
,l)+alpha2(3,6)*SIaaa2(i,j,k,l);

pppp42(i,j,k,l)=alpha2(4,1)*SII(i,j,k,l)+alpha2(4,4)*SIaa2(i,j,k,l)+alpha(4,7)*Saaaa2(i,j,k
,l)+alpha(4,8)*SIaaaa2(i,j,k,l);

          %Case1:Michigan State University model;
          pppp02(i,j,k,l)=C1*pppp12(i,j,k,l)+C2*pppp22(i,j,k,l);
        end
      end
    end
  end

  %Determine <pppp>:S
  for i=1:3
    for j=1:3
      M2(i,j)=0;
```

```
      for k=1:3
        for l=1:3
          M2(i,j)=M2(i,j)+pppp02(i,j,k,l)*s(l,k);
        end
      end
    end
  end

  %Determine <pp>:<pppp>
  for i=1:3
    for j=1:3
      N2(i,j)=0;
      for k=1:3
        for l=1:3
          N2(i,j)=N2(i,j)+pppp02(i,j,k,l)*a2(l,k);
        end
      end
    end
  end

  %Determine S.a+a.S, W.a+a.W(T);
  for i=1:3
    for j=1:3
      saas2(i,j)=0;
      waaw2(i,j)=0;
      for k=1:3
        saas2(i,j)=saas2(i,j)+s(i,k)*a2(k,j)+a2(i,k)*s(k,j);
        waaw2(i,j)=waaw2(i,j)+w(i,k)*a2(k,j)+a2(i,k)*w(j,k);
      end
    end
  end


  %Right handside of the equation
  for i=1:3
    for j=1:3
      dk3(i,j)=(ID(i,j)/3-a2(i,j))+lam*Pe*(saas2(i,j)-2*M2(i,j))-
Pe*waaw2(i,j)+U*(aa2(i,j)-N2(i,j));
    end
  end

  %3nd loop of 4th order R-K

  for i=1:3
    for j=1:3
      a3(i,j)=a(i,j)+dk3(i,j)*dt;
```

```
  end
end

%Determine S[I a];
for i=1:3
  for j=1:3
    for k=1:3
      for l=1:3
        SIa3(i,j,k,l)=ID(i,j)*a3(k,l)+ID(i,k)*a3(j,l)+ID(i,l)*a3(k,j);
        SIa3(i,j,k,l)=a3(i,j)*ID(k,l)+a3(i,k)*ID(j,l)+a3(i,l)*ID(k,j)+SIa3(i,j,k,l);
      end
    end
  end
end

%Determine S[a a];
for i=1:3
  for j=1:3
    for k=1:3
      for l=1:3
        Saa3(i,j,k,l)=a3(i,j)*a3(k,l)+a3(i,k)*a3(j,l)+a3(i,l)*a3(k,j);
      end
    end
  end
end

%Determine S[I(a*a)];
for i=1:3
  for j=1:3
    aa3(i,j)=0;
    bb3(i,j)=0;
    for k=1:3
      aa3(i,j) = aa3(i,j)+a3(i,k)*a3(k,j);
      bb3(i,j) = bb3(i,j)+(a3(i,k)-ID(i,k)/3)*(a3(k,j)-ID(k,j)/3);
    end
  end
end

for i=1:3
  for j=1:3
    for k=1:3
      for l=1:3
        SIaa3(i,j,k,l)=ID(i,j)*aa3(k,l)+ID(i,k)*aa3(j,l)+ID(i,l)*aa3(k,j);
        SIaa3(i,j,k,l)=aa3(i,j)*ID(k,l)+aa3(i,k)*ID(j,l)+aa3(i,l)*ID(k,j)+SIaa3(i,j,k,l);
      end
    end
```

```
  end
end

%Determine S[(a*a)a];
for i=1:3
  for j=1:3
    aa3(i,j)=0;
    for k=1:3
      aa3(i,j)=aa3(i,j)+a3(i,k)*a3(k,j);
    end
  end
end

for i=1:3
  for j=1:3
    for k=1:3
      for l=1:3
        Saaa3(i,j,k,l)=aa3(i,j)*a3(k,l)+aa3(i,k)*a3(j,l)+aa3(i,l)*a3(k,j);
        Saaa3(i,j,k,l)=a3(i,j)*aa3(k,l)+a3(i,k)*aa3(j,l)+a3(i,l)*aa3(k,j)+Saaa3(i,j,k,l);
      end
    end
  end
end

%Determine SIaaa;
for i=1:3
  for j=1:3
    aaa3(i,j)=0;
    bbb3(i,j)=0;
    for k=1:3
      aaa3(i,j)=aaa3(i,j)+aa3(i,k)*a3(k,j);
      bbb3(i,j)=bbb3(i,j)+bb3(i,k)*(a3(k,j)-ID(k,j)/3);
    end
  end
end


for i=1:3
  for j=1:3
    for k=1:3
      for l=1:3
        SIaaa3(i,j,k,l)=ID(i,j)*aaa3(k,l)+ID(i,k)*aaa3(j,l)+ID(i,l)*aaa3(k,j);
        SIaaa3(i,j,k,l) =
aaa3(i,j)*ID(k,l)+aaa3(i,k)*ID(j,l)+aaa3(i,l)*ID(k,j)+SIaaa3(i,j,k,l);
      end
    end
```

```
    end
  end

  %Determine S[(a*a)(a*a)];
  for i=1:3
    for j=1:3
      for k=1:3
        for l=1:3
          Saaaa3(i,j,k,l)=aa3(i,j)*aa3(k,l)+aa3(i,k)*aa3(j,l)+aa3(i,l)*aa3(k,j);
        end
      end
    end
  end


%Determine S[I(a*a*a*a)];
  for i =1:3
    for j=1:3
      aaaa3(i,j)=0;
      for k=1:3
        aaaa3(i,j)=aaaa3(i,j)+aaa3(i,k)*a3(k,j);
      end
    end
  end

  for i=1:3
    for j=1:3
      for k=1:3
        for l=1:3
          SIaaaa3(i,j,k,l)=ID(i,j)*aaaa3(k,l)+ID(i,k)*aaaa3(j,l)+ID(i,l)*aaaa3(k,j);

SIaaaa3(i,j,k,l)=aaaa3(i,j)*ID(k,l)+aaaa3(i,k)*ID(j,l)+aaaa3(i,l)*ID(k,j)+SIaaaa3(i,j,k,l);
        end
      end
    end
  end
  %Determine a:a (IIa) and alpha(2,1);
  IIa3=aa3(1,1)+aa3(2,2)+aa3(3,3);
  IIb3=bb3(1,1)+bb3(2,2)+bb3(3,3);
  alpha3(2,1)=2*(IIa3)/35;

  %Determine alpha(3,1);
  ALP13=aaa3(1,1)+aaa3(2,2)+aaa3(3,3);
  alpha3(3,1)=1/35+(4/35)*(ALP13/IIa3);
  IIIa3=aaa3(1,1)+aaa3(2,2)+aaa3(3,3);
  IIIb3=bbb3(1,1)+bbb3(2,2)+bbb3(3,3);
```

```
  %Determine alpha(3,4);
  alpha3(3,4)=1/(7*IIa3);

  %Determine alpha(3,5);
  alpha3(3,5)=1/IIa3;

  %Determine alpha(3,6);
  alpha3(3,6)=-4/(7*IIa3);

  %Determine alpha(4,1);
  ALP23=aaaa3(1,1)+aaaa3(2,2)+aaaa3(3,3);
  alpha3(4,1)=2/35*ALP23+(1/35)*IIa3*IIa3;

  %Determine alpha(4,4);
  alpha3(4,4)=(-1/7)*IIa3;


%MSU contribution;
  %Determine pppp1,pppp2
  for i=1:3
    for j=1:3
      for k=1:3
        for l=1:3
          pppp53(i,j,k,l)=a3(i,j)*a3(k,l);
          pppp13(i,j,k,l)=alpha(1,1)*SII(i,j,k,l)+alpha(1,2)*SIa3(i,j,k,l);

%pppp2(i,j,k,l)=alpha(2,1)*SII(i,j,k,l)+alpha(2,2)*SIa(i,j,k,l)+alpha(2,3)*Saa(i,j,k,l)+alp
ha(2,4)*SIaa(i,j,k,l);

pppp23(i,j,k,l)=alpha3(2,1)*SII(i,j,k,l)+alpha(2,3)*Saa3(i,j,k,l)+alpha(2,4)*SIaa3(i,j,k,l);

          %Case1:Michigan State University model;
          pppp03(i,j,k,l)=C1*pppp13(i,j,k,l)+C2*pppp23(i,j,k,l);
        end
      end
    end
  end

  %Determine <pppp>:S
  for i=1:3
    for j=1:3
      M3(i,j)=0;
      for k=1:3
        for l=1:3
          M3(i,j)=M3(i,j)+pppp03(i,j,k,l)*s(l,k);
```

```
      end
    end
  end
end

%Determine <pp>:<pppp>
for i=1:3
  for j=1:3
    N3(i,j)=0;
    for k=1:3
      for l=1:3
        N3(i,j)=N3(i,j)+pppp03(i,j,k,l)*a3(l,k);
      end
    end
  end
end

%Determine S.a+a.S, W.a+a.W(T);
for i=1:3
  for j=1:3
    saas3(i,j)=0;
    waaw3(i,j)=0;
    for k=1:3
      saas3(i,j)=saas3(i,j)+s(i,k)*a3(k,j)+a3(i,k)*s(k,j);
      waaw3(i,j)=waaw3(i,j)+w(i,k)*a3(k,j)+a3(i,k)*w(j,k);
    end
  end
end


%Right handside of the equation
for i=1:3
  for j=1:3
    dk4(i,j)=(ID(i,j)/3-a3(i,j))+lam*Pe*(saas3(i,j)-2*M3(i,j))-
Pe*waaw3(i,j)+U*(aa3(i,j)-N3(i,j));
  end
end

%4nd loop of 4th order R-K

for i=1:3
  for j=1:3

    %Overall computation
    a(i,j)=a(i,j)+(1/6)*(dk1(i,j)+2*dk2(i,j)+2*dk3(i,j)+dk4(i,j))*dt;
    E=[a(1,1),a(1,2),a(1,3);a(2,1),a(2,2),a(2,3);a(3,1),a(3,2),a(3,3)];
```

```
[v,lambdal]=eig(E);

if i==2
  if j==3
    A(n)=a(i,j);
    time(n)=(n-1)*dt;
  end
end
if i==2
  if j==2
    B(n)=a(i,j);
    time(n)=(n-1)*dt;
  end
end
if i==1
  if j==1
    C(n)=a(i,j);
    time(n)=(n-1)*dt;
  end
end
if i==3
  if j==3
    D(n)=a(i,j);
    time(n)=(n-1)*dt;
  end
end


%d(n)=det(E);
e3(n)=v(3,3);
time(n)=(n-1)*dt;
e2(n)=v(2,2);
time(n)=(n-1)*dt;
en(n)=v(2,3);
time(n)=(n-1)*dt;
e1(n)=v(1,1);
time(n)=(n-1)*dt;
l2(n)=lambdal(2,2);
time(n)=(n-1)*dt;
l3(n)=lambdal(3,3);
time(n)=(n-1)*dt;
l1(n)=lambdal(1,1);
time(n)=(n-1)*dt;

if i==1
  if j==1
```

```
        BB(n)=bb(i,j);
        BBB(n)=bbb(i,j);
      end
    end
    if i==2
      if j==2
        CC(n)=bb(i,j);
        CCC(n)=bbb(i,j);
      end
    end
    if i==3
      if j==3
        DD(n)=bb(i,j);
        DDD(n)=bbb(i,j);
      end
    end
  end
end

for i=1:3
  for j=1:3
    II(n)=BB(n)+CC(n)+DD(n);
    III(n)=BBB(n)+CCC(n)+DDD(n);
  end
end

a

%Computation of finding tau values

  %Determine S[I a];
  for i=1:3
    for j=1:3
      for k=1:3
        for l=1:3
          SIatau(i,j,k,l)=ID(i,j)*a(k,l)+ID(i,k)*a(j,l)+ID(i,l)*a(k,j);
          SIatau(i,j,k,l)=a(i,j)*ID(k,l)+a(i,k)*ID(j,l)+a(i,l)*ID(k,j)+SIatau(i,j,k,l);
        end
      end
    end
  end

  %Determine S[a a];
  for i=1:3
    for j=1:3
      for k=1:3
```

```
        for l=1:3
          Saatau(i,j,k,l)=a(i,j)*a(k,l)+a(i,k)*a(j,l)+a(i,l)*a(k,j);
        end
      end
    end
  end

  %Determine S[I(a*a)];
  for i=1:3
    for j=1:3
      aatau(i,j)=0;
      bbtau(i,j)=0;
      for k=1:3
        aatau(i,j) = aatau(i,j)+a(i,k)*a(k,j);
        bbtau(i,j) = bbtau(i,j)+(a(i,k)-ID(i,k)/3)*(a(k,j)-ID(k,j)/3);
      end
    end
  end


  for i=1:3
    for j=1:3
      for k=1:3
        for l=1:3
          SIaatau(i,j,k,l)=ID(i,j)*aatau(k,l)+ID(i,k)*aatau(j,l)+ID(i,l)*aatau(k,j);

SIaatau(i,j,k,l)=aatau(i,j)*ID(k,l)+aatau(i,k)*ID(j,l)+aatau(i,l)*ID(k,j)+SIaatau(i,j,k,l);
        end
      end
    end
  end

  %Determine S[(a*a)a];
  for i=1:3
    for j=1:3
      aatau(i,j)=0;
      for k=1:3
        aatau(i,j)=aatau(i,j)+a(i,k)*a(k,j);
      end
    end
  end

  for i=1:3
    for j=1:3
      for k=1:3
        for l=1:3
```

```
          Saaatau(i,j,k,l)=aatau(i,j)*a(k,l)+aatau(i,k)*a(j,l)+aatau(i,l)*a(k,j);

Saaatau(i,j,k,l)=a(i,j)*aatau(k,l)+a(i,k)*aatau(j,l)+a(i,l)*aatau(k,j)+Saaatau(i,j,k,l);
        end
      end
    end
  end

  %Determine SIaaa;
  for i=1:3
    for j=1:3
      aaatau(i,j)=0;
      bbbtau(i,j)=0;
      for k=1:3
        aaatau(i,j)=aaatau(i,j)+aatau(i,k)*a(k,j);
        bbbtau(i,j)=bbbtau(i,j)+bbtau(i,k)*(a(k,j)-ID(k,j)/3);
      end
    end
  end



for i=1:3
    for j=1:3
      for k=1:3
        for l=1:3
          SIaaatau(i,j,k,l)=ID(i,j)*aaatau(k,l)+ID(i,k)*aaatau(j,l)+ID(i,l)*aaatau(k,j);

SIaaatau(i,j,k,l)=aaatau(i,j)*ID(k,l)+aaatau(i,k)*ID(j,l)+aaatau(i,l)*ID(k,j)+SIaaatau(i,j,k,
l);
        end
      end
    end
  end

  %Determine S[(a*a)(a*a)];
  for i=1:3
    for j=1:3
      for k=1:3
        for l=1:3
          Saaaatau(i,j,k,l)=aatau(i,j)*aatau(k,l)+aatau(i,k)*aatau(j,l)+aatau(i,l)*aatau(k,j);
        end
      end
    end
  end
```

```
  %Determine S[I(a*a*a*a)];
  for i =1:3
    for j=1:3
      aaaatau(i,j)=0;
      for k=1:3
        aaaatau(i,j)=aaaatau(i,j)+aaatau(i,k)*a(k,j);
      end
    end
  end

  for i=1:3
    for j=1:3
      for k=1:3
        for l=1:3
          SIaaaatau(i,j,k,l)=ID(i,j)*aaaatau(k,l)+ID(i,k)*aaaatau(j,l)+ID(i,l)*aaaatau(k,j);

SIaaaatau(i,j,k,l)=aaaatau(i,j)*ID(k,l)+aaaatau(i,k)*ID(j,l)+aaaatau(i,l)*ID(k,j)+SIaaaatau
(i,j,k,l);
        end
      end
    end
  end

%Determine a:a (IIa) and alpha(2,1);
  IIatau=aatau(1,1)+aatau(2,2)+aatau(3,3);
  IIbtau=bbtau(1,1)+bbtau(2,2)+bbtau(3,3);
  alphatau(2,1)=2*IIatau/35;

  %Determine alpha(3,1);
  ALP1tau=aaatau(1,1)+aaatau(2,2)+aaatau(3,3);
  alphatau(3,1)=1/35+(4/35)*(ALP1tau/IIatau);
  IIIatau=aaatau(1,1)+aaatau(2,2)+aaatau(3,3);
  IIIbtau=bbbtau(1,1)+bbbtau(2,2)+bbbtau(3,3);

  %Determine alpha(3,4);
  alphatau(3,4)=-1/(7*IIatau);

  %Determine alpha(3,5);
  alphatau(3,5)=1/IIatau;

  %Determine alpha(3,6);
  alphatau(3,6)=-4/(7*IIatau);

  %Determine alpha(4,1);
  ALP2tau=aaaatau(1,1)+aaaatau(2,2)+aaaatau(3,3);
  alphatau(4,1)=2/35*ALP2tau+(1/35)*IIatau*IIatau;
```

```
  %Determine alpha(4,4);
  alphatau(4,4)=(-1/7)*IIatau;


  %MSU contribution;
  %Determine pppp1,pppp2,pppp3,pppp4;
  for i=1:3
    for j=1:3
      for k=1:3
        for l=1:3
          pppp5tau(i,j,k,l)=a(i,j)*a(k,l);
          pppp1tau(i,j,k,l)=alpha(1,1)*SII(i,j,k,l)+alpha(1,2)*SIatau(i,j,k,l);

%pppp2(i,j,k,l)=alpha(2,1)*SII(i,j,k,l)+alpha(2,2)*SIa(i,j,k,l)+alpha(2,3)*Saa(i,j,k,l)+alp
ha(2,4)*SIaa(i,j,k,l);

pppp2tau(i,j,k,l)=alphatau(2,1)*SII(i,j,k,l)+alpha(2,3)*Saatau(i,j,k,l)+alpha(2,4)*SIaatau(
i,j,k,l);



%Case1:Michigan State University model;
          pppp0tau(i,j,k,l)=C1*pppp1tau(i,j,k,l)+C2*pppp2tau(i,j,k,l);
        end
      end
    end
  end

  %Determine <pppp>:S
  for i=1:3
    for j=1:3
      Mtau(i,j)=0;
      for k=1:3
        for l=1:3
          Mtau(i,j)=Mtau(i,j)+pppp0tau(i,j,k,l)*s(l,k);
        end
      end
    end
  end

  %Determine <pp>:<pppp>
  for i=1:3
    for j=1:3
      Ntau(i,j)=0;
      for k=1:3
```

```
      for l=1:3
        Ntau(i,j)=Ntau(i,j)+ppppOtau(i,j,k,l)*a(l,k);
      end
    end
  end
end


%Computation of tau
for i=1:3
  for j=1:3

    tau(i,j)=(a(i,j)-1/3*ID(i,j))-U*(aa(i,j)-N(i,j))+Pe*M(i,j);

    if i==2
      if j==3
        W(n)=tau(i,j);
        time(n)=(n-1)*dt;
      end
    end
    if i==2
      if j==2
        X(n)=tau(i,j);
        time(n)=(n-1)*dt;
      end
    end
    if i==1
      if j==1
        Y(n)=tau(i,j);
        time(n)=(n-1)*dt;
      end
    end
    if i==3
      if j==3
        Z(n)=tau(i,j);
        time(n)=(n-1)*dt;
      end
    end
  end
end

%Primary normal stress
for i=1:3
  for j=1:3
    P(n)=Z(n)-X(n);
  end
```

```
  end

  %Secondary normal stress
  for i=1:3
    for j=1:3
      Q(n)=X(n)-Y(n);
    end
  end

  %Time average
  f(1)=0;
  f(n+1)=f(n)+1;
  R(n)=0;
  if all(f(n)>limitn1) & all(f(n)<limitn2)
    R(n)=P(n);
  end
end

averagetau=sum(R)/round(limitn2-limitn1-1)
mean(P(n))


xIII=[-1/36:0.0001:2/9];
yII=2/9+2*xIII;

yyII=[0:0.0001:1/6];
xxIII=-6*(yyII/6).^(3/2);

yyyII=[0:0.0001:2/3];
xxxIII=6*(yyyII/6).^(3/2);

Smin=[-.04 :0.01: 0.05];
Smax=[0.1 0.15 .2];
IIbmin=[.0816 .0816 .0816 .0816 .0816 .0816 .0816 .0816 .0816 .0816];
IIbmax=[.552067 .552067 .552067];

%plot(xIII,yII,xxIII,yyII,xxxIII,yyyII,III,II,':',Smin,IIbmin,'--',Smax,IIbmax,'--
'),xlabel('IIIb'),ylabel('IIb');
%plot(xIII,yII,xxIII,yyII,xxxIII,yyyII,III,II,'+'),xlabel('IIIb'),ylabel('IIb'),axis([.2 .24 .6
.68]);
%plot(xIII,yII,xxIII,yyII,xxxIII,yyyII,III,II,'-.'),xlabel('IIIb'),ylabel('IIb');
%curve D
%plot(xIII,yII,xxIII,yyII,xxxIII,yyyII,III,II,':',-
0.0113,0.0915,'o',0,0,'square'),xlabel('IIIb'),ylabel('IIb'),axis([-.03 .001 -0.05 .2]);
%curve B
```

```
%plot(xIII,yII,xxIII,yyII,xxxIII,yyyII,III,II,':',-
0.0113,0.0915,'o',0,0,'square'),xlabel('IIIb'),ylabel('IIb'),axis([-.05 .25 0.15 .68]);
%curve F
%plot(xIII,yII,xxIII,yyII,xxxIII,yyyII,III,II,':',-
0.0113,0.0915,'o',0,0,'square'),xlabel('IIIb'),ylabel('IIb'),axis([-.01 .25 0 .67]);
%plot(time,ev22)
%plot(time,d,'*'),xlabel('det of b'),ylabel('t')
%a(2,3)
% E
%v
%lambdal(3)
%e3
% IIb
% IIIb


%aij curve
%plot(time,A,time,e3,'-.',time,D,'--',time,en,':'),xlabel('t'),ylabel('aij')
%  maxlam=1.5*e3-0.5;
%  plot(time,A,time,maxlam,'-.',time,D,'--',time,en,':'),xlabel('Time'),ylabel('Alpha')

%eigan director curves
%plot(time,e3,'--',time,e2,':',time,en,'-.'),xlabel('t'),ylabel('vij'),axis([0 15 -1.2 1.2])
%plot(time,l3,time,e3,'--'),xlabel('t'),ylabel('vij')

%eigan value curves
%plot(time,l2,'-.',time,l3,'--',time,l1),xlabel('t'),ylabel('lambdal')
%plot(time,en,'+')

%stress tensor tau curves
%plot(time,W,time,X,'-.',time,Y,':',time,Z,'--'),xlabel('t'),ylabel('tauij')

%Primary and Secondary stress curves
%plot(time,P,time,Q,':'),xlabel('t'),ylabel('normal stress');
```

LIST OF REFERENCES

Advani, S.G. and C.L. Tucker III, 1987, " The Use of Tensors to Describe and Predict Fiber Orientation in Short Fiber Composites ", *J. Rheol.*, **31** (8), 751-784.

Advani, S.G., and C.L. Tucker III, 1990, " Closure Approximations for Three-Dimensional Structure Tensors " , *J. Rheol.*, **34** (3), 367-386

Aharoni, S.M., 1979, " Rigid Backbone Polymers, 2: Polyisocyanates and Their Liquid – Crystal Behavior " *Macromolecules*, **12**, 94-103.

Aharoni, S. M., and E. K. Walsh , 1979, " Rigid Backbone Polymers. 4. Solution Properties of Two Lyotropic Mesomorphic Poly(isocyanates)" *Am. Chem. Soc.*, **12(2)**, 271-276.

Aharoni, S.M., 1980, " Rigid Backbone Polymers, XVII: Solution Viscosity of Polydisperse Systems, *Polymer*, **21**, 1413-1422.

Bhave, A.V., R.K. Menon, R.C. Armstrong, and R.A. Brown, 1993 "A Constitutive Equation for Liquid-Crystalline Polymer Solutions", *J.Rheol.*, **37**(3), 413-441.

Chaubal, C.V., L.G. Leal and G.H. Fredrickson, 1995, "A Comparison of Closure Approximations for the Doi Theory of LCPs", *J.Rheol.*, **39**(1), 73-104.

Cintra, J.S. and C.L. Tucker III, 1995, " Orthotropic Closure Approximations for Flow-Induced Fiber Orientation ", *J. Rheol.*, **39** (6), 1095-1122.

Collings, C.J. and J.S. Patel, 1997, *Handbook of Liquid Crystal Research*, Oxford University Press, London.

Deen, W., 1998, *Ananlysis of Transport Phenomena*, Oxford University Press, New York.

Doi, M, 1981, "Molecular Dynamics and Rheologoial Properties of Concentrated Solutions of Rodlike Polymers in Isotropic and Liquid Crystalline Phases", *J.Poly. Sci Polym.Phy.Ed.*, **19**, 229-243.

Doi, M. and S.F. Edwards, 1986, *Theory of Polymer Dynamics*, Oxford University Press, London.

Feng, J., C. V. Chaubal, and L.G. Leal, 1998, " Closure Approximations for the Doi Theory: Which to Use in Simulating Complex Flows of Liquid-Crystalline Polymers ", J. Rheol., **42**(5), 1095-1119.

Folgar, F. and C.L. Tucker III, 1984, " Orientation Behavior of Fibers in Concentrated Suspensions ", *J. Reinf. Plast. Compos.*, 98-119.

Hand, G.L., 1962, " A Theory of Anisotropic Fluids ", *J. Fluid Mech.*, **13**, 33-46.

Hinch, E.J. and L.G. Leal, 1975, " Constitutive Equations in Suspension Mechanics. Part 1. General Formulation ", *J. Fluid Mech.*, Vol. 71, Part 3, 481-495.

Hinch, E.J. and L.G. Leal, 1976, " Constitutive Equations in Suspension Mechanics. Part 2. Approximate Forms for a Suspension of Rigid Particles Affected by Brownian Rotations ", *J. Fluid Mech.*, Vol. 76, Part 1, 187-208.

Imhoff, A., 2000, Mechanical Engineering, Diplomarbeit: *Validation of Closure Models for Fiber Induced Alignment of Fibers*, Michigan State University/University of Aachen, 2000

Jeffery, G.B., 1922, " The Motion of Ellipsoidal Particles Immersed in Viscous Fluid ", *Proc. R. Soc. Lond. A*, **102**, 161-179.

Kini, H.K., Y.C.Kim, C.T. Nguyen, A. Bénard, and C. A. Petty, 2003, "Flow Induced Microstructure in Composite Materials", Proceedings of the 14th International Conference on Composite Materials, ICCM14 CD-ROM, San Diego, California
July 14-18, 2003

Larson, R.G., 1999, *The Structure of Complex Fluids,* Oxford University Press, London.

Nguyen, C. T. 2001, *Molecular Orientation of Liquid Crystalline Polymers Under Simple Shear Flows,* MS Thesis, Michigan State University

Parks S. M., C. A. Petty, and M. Shafer, 1999, " Flow-Induced Alignment of Fibers in the Absence of Fiber-Fiber Interactions ", paper presentation, *Symposium on Suspensions*, APS/DFD, New Orleans, LA, November 21-23.

Petty C. A., S. M. Parks, and S. M. Shao , 1999, " Flow Induced Alignment of Fibers ", in Proceedings of *12th International Conference on Composite Materials*, ICCM12/TCA, Paris, July 5-9.

Rey, A.D. and M.M. Denn, 2002, "Dynamical Phenomena in Liquid-Crystalline Materials", *Annual Review of Fluid Mechanics*, **34**, 233-266.

Tucker, C.L., 1988, " Predicting Fiber Orientations in Short Fiber Composites ", p.95 in *Proc. Manufacturing Int'l*, AMSE Publication, New York.

Tucker III, C.L. and S.G. Advani, 1994, " Processing of Short-Fiber Systems ", pp. 147-202, in *Flow and Rheology in Polymer Composites Manufacturing,* Volume 10, Composite Materials Series, Editor: S.G. Advani, Elsevier

Weiss R. A. and C. K. Ober, 1990, " Current Topics in Liquid-Crystalline Polymers " , pp 1-13, in *Liquid Crystalline Polymers* , ACS Symposium Series 435, American Chemical Society, Washington, DC, Edited by : R. A.Weiss and C. K. Ober